CHAPTER 5: II-VI COMPOUND SEMICONDUCTORS

The II-VI compound semiconductors are materials exhibiting various interesting solid-state phenomenon of great significance because of its developments in the field of optoelectronics and scientific applications. Zinc sulphide (ZnS), Cadmium Telluride (CdTe) and Zinc Selenide (ZnSe) are II-VI compound semiconductor having wide band gap. They are found to crystallize in zinc-blende (ZB) and wurzite (WZ) structure under ambient pressure conditions. In various studies, a phase transition from four-fold co-ordinated zinc-blende (ZB) to six-fold co-ordinated rock-salt (RS) has been reported at elevated pressure.

Detail literature review on the available research papers have been discussed in chapter 2.

The primary aim of the work in this chapter is to perform a detailed study on the structural stability and phase transition from zincblende (ZB) to rocksalt (RS) phase of ZnS, CdTe and ZnSe as well as the effects of pressure in the elastic properties and electronic structures of these compounds.

5.1. Structural Properties and Phase transition

The static equilibrium properties of the crystal structure of ZB and RS of ZnS, CdTe and ZnSe are obtained by minimization of the total energy with respect to the unit cell volumes per molecule and fitting it to the Birch–Murnaghan equation [81]. As discussed in III-V compounds, the structural phase transition has been calculated from the condition of equal enthalpies, H=E+PV. Since our calculation is done at zero temperature we have ignored the entropy contribution.

In the following, the structural properties and phase transition of II-VI compound semiconductors: ZnS, CdTe and ZnSe are discussed. In all calculations, we have used LDA and GGA exchange correlations to see the comparative results.

(a) Zinc Sulfide (ZnS)

For the structural optimization of ZnS (in ZB and RS structure), the total energy as a function of volume with LDA and GGA as exchange correlation are shown in figure 5.1(a-b). From the figures, it is observed that ZnS in ZB structure has lower total energy at the equilibrium volume in both the methods thus indicating that the ZnS-ZB structure is more stable than the ZnS-RS structure.

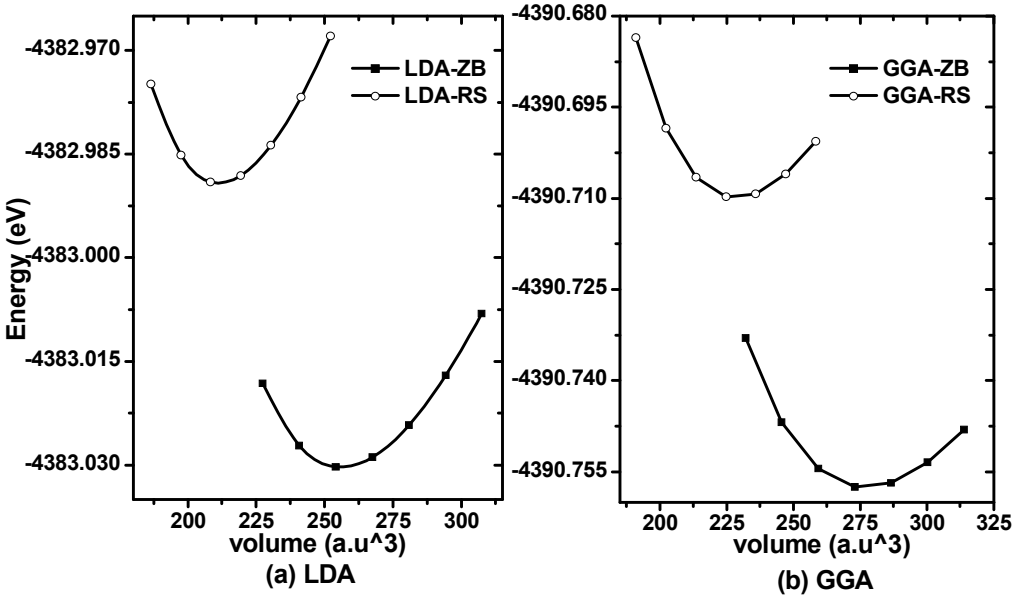

Figure 5.1. Total energy as a function of primitive cell volume for ZnS-ZB and ZnS-RS with (a) LDA and (b) GGA

Table 5. 1. Experimental and calculated ground state structural parameters of ZnS in ZB and RS structure

		Zinc Blende (ZB) Strucutre			**Rock Salt (RS) Structure**		
		a_0 (A^0)	B_0 (GPa)	$B^/$	a_0 (A^0)	B_0 (GPa)	$B^/$
Present work	LDA	5.336	88.88	4.62	5.004	111.75	4.83
	GGA	5.475	71.75	4.51	5.135	88.73	4.83
Expt. work		5.412[a], 5.410[k]	75[a], 76.9[k],	4.4[f], 4.9[k]	5.06[h], 5.13[j]	103.6[h], 85.01[j]	4.00[h]
Other theo. calculation		5.328[b], 5.335[c], 5.342[d]	83.8[b], 83.70[c], 89.67[d], 77.1[e]	4.48[g], 4.05[h],	5.066[i]	100.1[h]	4.05[h] ,

[a]Ref[127], [b]Ref[128], [c]Ref[129], [d]Ref[130], [e]Ref[131], [f]Ref[132], [g]Ref[39], [h]Ref[37], [i]Ref[42], [j]Ref[133], [k]Ref[134]

The calculated ground state structural parameters of ZnS-ZB and ZnS-RS are given in table 5.1 and compared with other available experimental and theoretical data.

For the stable ZnS-ZB phase, the experimental lattice parameter within the LDA shows a difference of 1.40% while that of GGA shows a difference of 1.16% which is quite acceptable within 2% difference. Thus our results are in good agreement with other studies and are used for further calculation of phase transition and energy band structure.

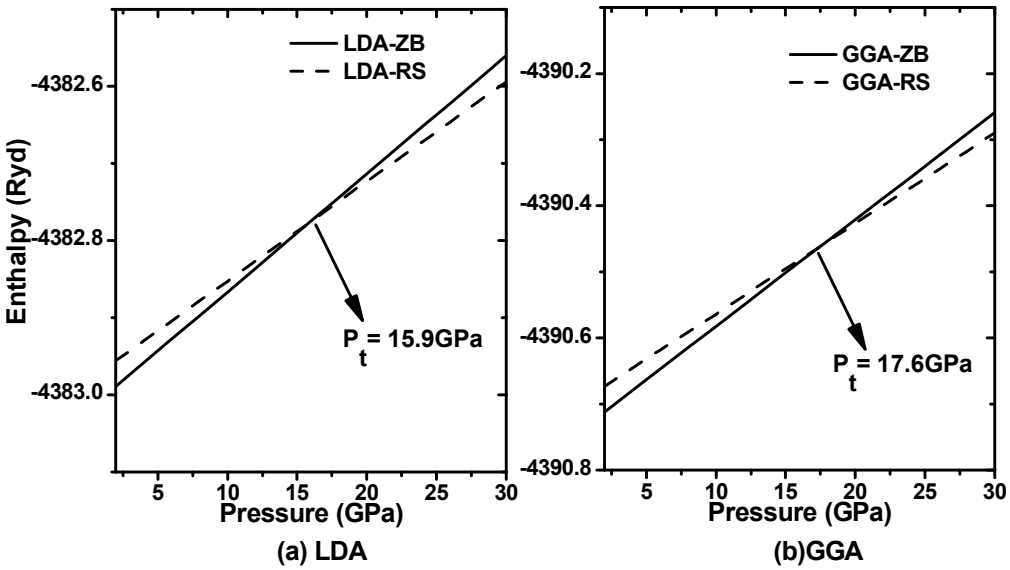

Figure 5.2. Enthalpy as a function of pressure of ZnS-ZB and ZnS-RS phase within (a) LDA and (b) GGA

Table 5.2. Phase transition pressure 'P_t(GPa)' and volume collapse of ZnS.

	Present calculation	**Expt. Results**	**Theoretical results**
Transition pressure (P_t)(GPa)	15.9 (LDA) 17.6 (GGA)	18.1[a],16.9[b],	14.35[c], 14.5[d], 17.4[e], 17.5[f]
Volume collapse (%)	12.86		-

[a]Ref[135], [b]Ref[41], [c]Ref[50], [d]Ref[136], [e]Ref[137], [f]Ref[138],

The phase transition under induced pressure is the pressure at which both the phases have equal Enthalpy. The plot of Enthalpy as a function of various pressures of both the phases is shown in figure 5.2. From the figure we see the transformation from ZnS-ZB to ZnS-RS within the LDA calculation occurs at 15.9 GPa pressure while the transition within the GGA calculation is at 17.6 GPa pressure. As GGA gives us better result of phase transition, we have calculated the volume collapse of ZnS within the GGA only as shown in figure 5.3. Figure 5.3 shows normalised volume (Vp/Vo) as a function of pressure. During the phase transition, the normalised volume of ZB and RS phase is 0.845 and 0.716 respectively with a volume decrease of 12.86% indicating that the ZB phase is more compressible than the RS phase. The

phase transition parameters of the present work are compared with other experimental and theoretical results in table 5.2.

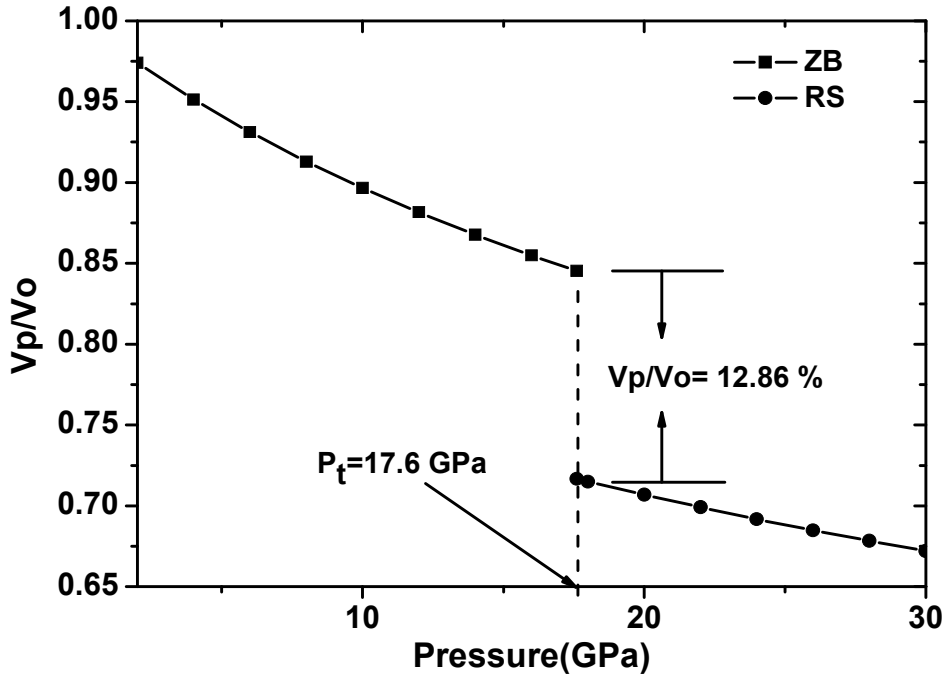

Figure 5.3. Normalized volume as a function of pressure for ZnS-ZB and ZnS-RS

(b) Cadmium Telluride (CdTe)

Following the same methods of calculations as before, the results of structural properties and phase transition of CdTe are discussed in this sub section.

For structure optimization, the total energy as a function of volume of CdTe of both the ZB and RS phase within LDA and GGA are shown in figure 5.4. The lower total energy at the equilibrium volume in both LDA and GGA method indicates the CdTe-ZB structure is more stable than the RS structure. The structural parameters of present work and the experimental data along with other calculations available in the relevant literatures are given in table 5.3

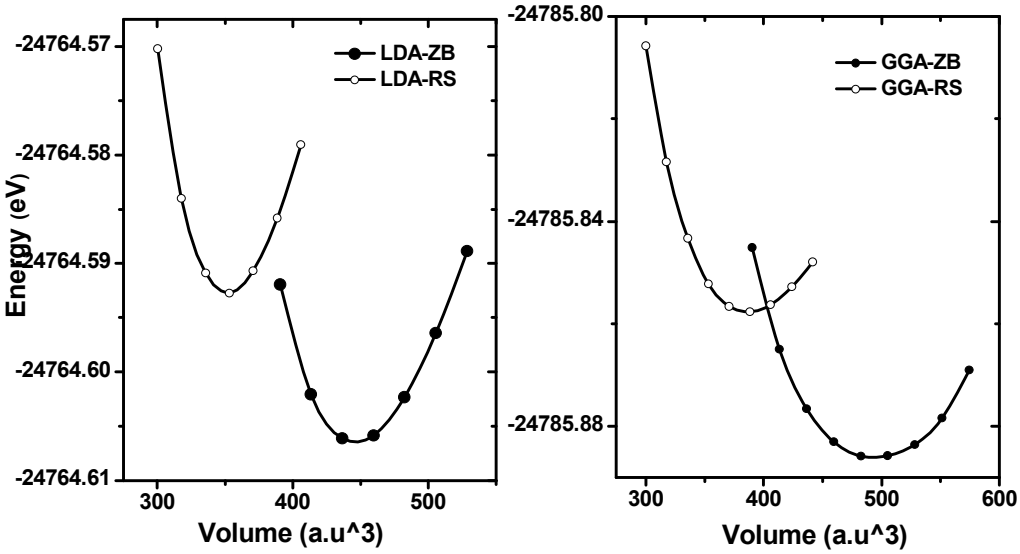

Figure 5.4. Total energy as a function of volume of CdTe- ZB and CdTe-RS structure with LDA and GGA methods

Table 5.3. Experimental and calculated ground state structural parameters of CdTe

		Zinc Blende (ZB) Strucutre			**Rock Salt (RS) Structure**		
		a_0 (A^0)	B_0 (GPa)	$B^/$	a_0 (A^0)	B_0 (GPa)	$B^/$
Present work	LDA	6.42	47.67	5.05	5.92	63.82	5.01
	GGA	6.65	25.28	8.35	6.11	48.24	4.99
Expt. work		6.53[a], 6.49[b]	42[g], 45[h]	6.4[g]	-	-	-
Other Theo. Calculation		6.63[c], 6.62[d], 6.58[e]	33.8[c], 39.0[d], 36.6[e]	5.26[c], 5.14[c], 4.6[d]	6.11[d], 5.94[d], 5.9[f]	56.0[d], 66.4[f]	4.3[d], 5.1[d], 4.67[i]

[a]Ref[139], [b]Ref[140], [c]Ref[141], [d]Ref[142], [e]Ref[143], [f]Ref[144], [g]Ref[145], [h]Ref[146], [i]Ref[147].

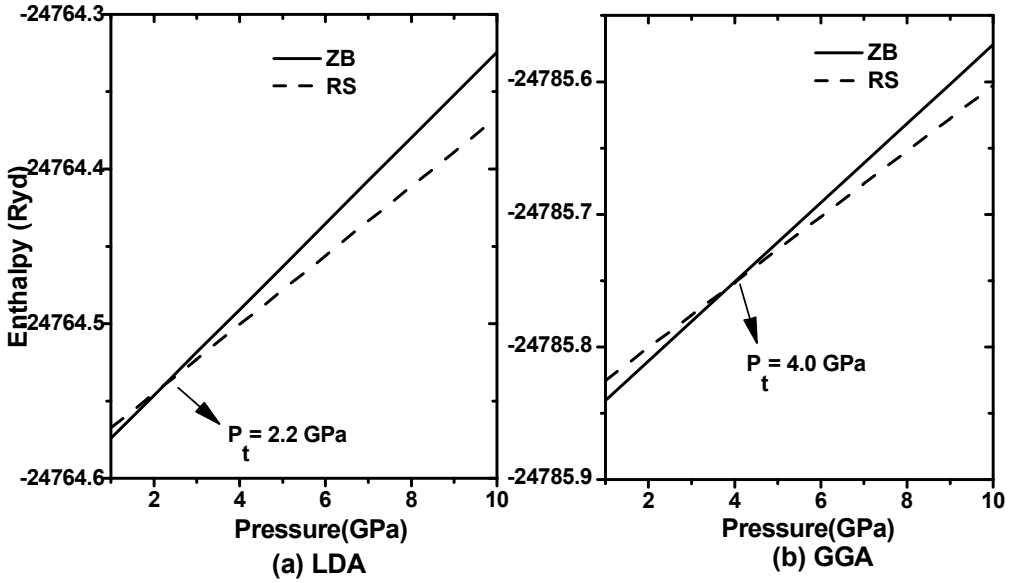

Figure 5.5. Enthalpy as a function of pressure for ZB and RS phase of CdTe with (a) LDA method and (b) GGA method

Table 5. 4. Phase transition pressure and volume collapse of CdTe.

	Present calculation	**Expt. results**	**Theoretical results**
Phase Transition pressure(P_t) (GPa)	2.2 (LDA) 4.0 (GGA)	3.9[a],3.8[b], 3.8[c],3.8[d]	4.0[e], 3.9[f]
Volume collapse (%)	20.9	-	19.0[b], 19.0[e]

[a]Ref[137], [b]Ref[148], [c]Ref[149], [d]Ref[150], [e]Ref[151], [f]Ref[152].

Figure 5.5 shows the phase transition of CdTe-ZB to CdTe-RS at 2.2 GPa with LDA method and at 4.0 GPa pressure with GGA calculation. Table 5.4 shows that the transition pressure obtained with GGA method is more accurate as compare to the available experimental data and hence volume collapse is calculated using GGA method as given in figure 5.6. During the phase transition the normalised volume of the CdTe-ZB and Cd-Te-RS phase is 0.90 and 0.69 respectively with a volume reduction of 20.9% indicating that the ZB phase is more compressible than the RS phase.

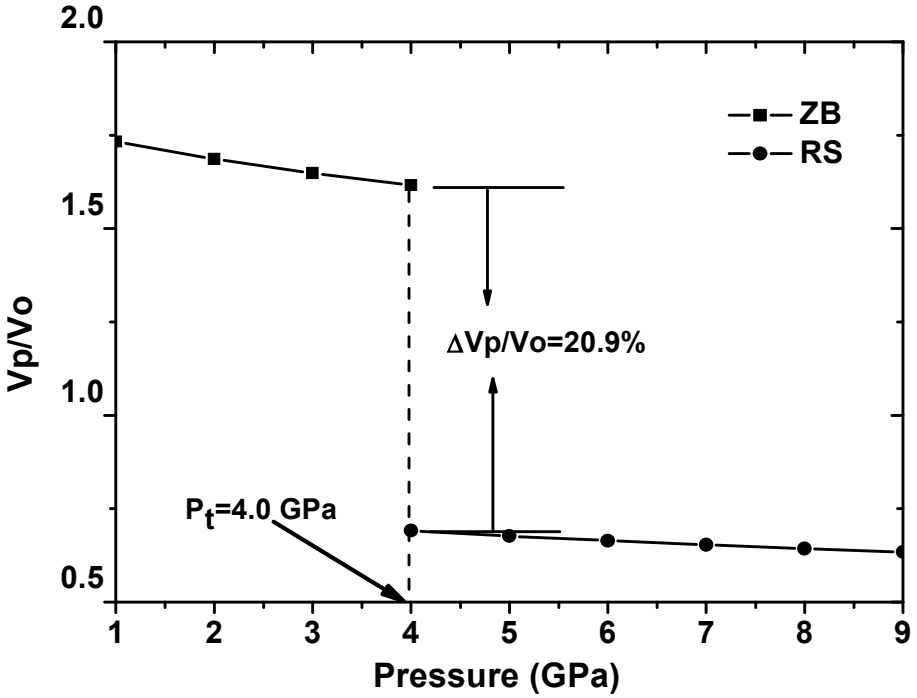

Figure 5.6. Normalised volume versus pressure of CdTe-ZB and CdTe-RS structure within GGA

(c) Zinc Selenide (ZnSe)

The results of the structural properties and the phase transition of ZnSe as obtained in the same methodology as discussed above are explained in brief in this subsection.

In case of ZnSe also, the ZnSe-ZB structure is found to be more stable than ZnSe-RS structure as observed the lower total energy at the equilibrium volume in both LDA and GGA methods as shown in figure 5.7. The structural parameters of ZnSe-ZB and ZnSe-RS of present work are compared with other experimental and theoretical data in table 5.5.

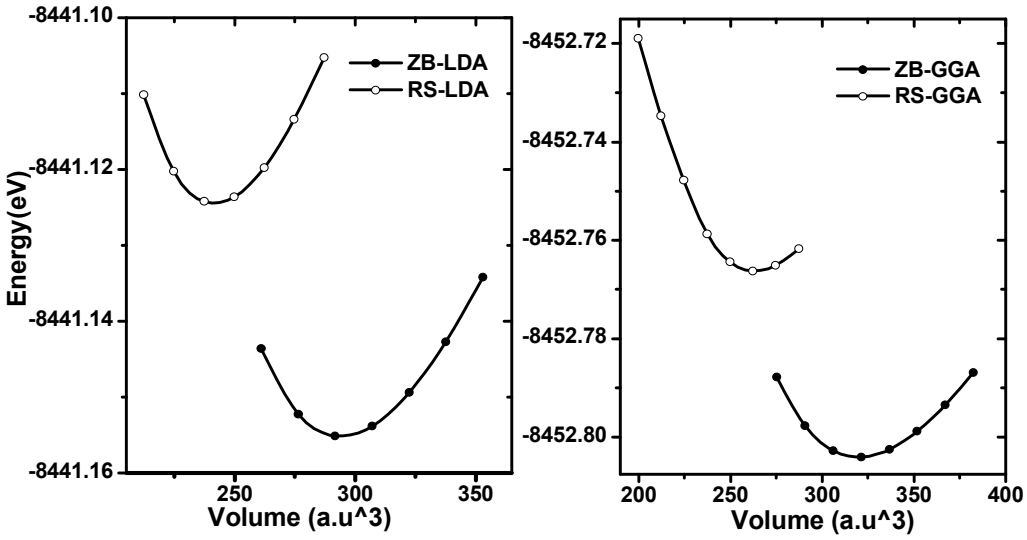

Figure 5.7. Total energy as a function of volume of ZnSe -ZB and ZnSe-RS structure within LDA and GGA methods.

Table 5.5. Experimental and calculated ground state structural parameters of ZnSe in ZB and RS structure

		Zinc Blende (ZB) Strucutre			**Rock Salt (RS) Structure**		
		a_0 (A^0)	B_0 (GPa)	$B^/$	a_0 (A^0)	B_0 (GPa)	$B^/$
Present work	LDA	5.58	73.40	4.70	5.23	91.84	4.87
	GGA	5.74	57.89	4.48	5.38	71.27	4.78
Expt. work		5.66[a],	64.7[a]	4.77[a]	5.66[b]	104[b]	4.0 [b]
Other Theo. Calculation		5.75 [c], 5.63[d]	57.30[c], 68.9 [d]	4.56 [c], 4.36 [d]	5.38[c], 5.26[d]	75.59[c], 88.5[d]	3.60[c], 4.28[d]

[a]Ref[153], [b]Ref[154], [c]Ref[155], [d]Ref[50]

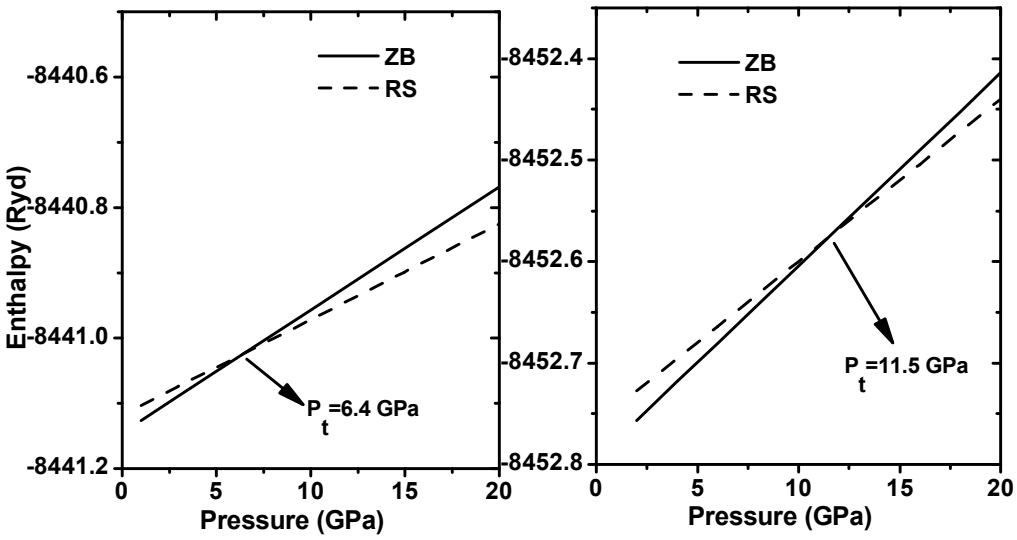

Figure 5.8. Enthalpy as a function of pressure for ZB and RS phase of ZnSe with (a) LDA method and (b) GGA method

Table 5.6. Phase transition pressure 'P_t(GPa)' and volume collapse of ZnSe

	Present calculation	**Expt. results**	**Theoretical results**
Transition pressure (P_t)(GPa)	6.4 (LDA) 11.5 (GGA)	13.0±0.5[a],11.8±0.5[b], 13.0[c]	9.95[d], 15[e], 13.7[f],
Volume collapse (%)	13.74	15.2[c]	-

[a]Ref[156], [b]Ref[157], [c]Ref[158], [d]Ref[10], [e]Ref[159], [f]Ref[52]

The structural phase transition pressure of ZnSe-ZB to ZnSe-RS is obtained at equal enthapy from the plot of enthalpy versus pressure in figure 5.7. The phase transition pressures as obtained with LDA and GGA are given in table 5.6. As the transition pressure obtained with GGA is more accurate to LDA as compare to experimental results, we calculate volume collapse with GGA method. As shown in figure 5.9, during the phase transition, the normalised volume of ZnSe-ZB are found to be 0.866 and that of ZnSe-RS phase is 0.728 with a volume decrease of 13.74%. It means that ZB phase is more compressible than the RS phase. The present results of the calculated volume collapse are compared with other experimental and theoretical results in table 5.6.

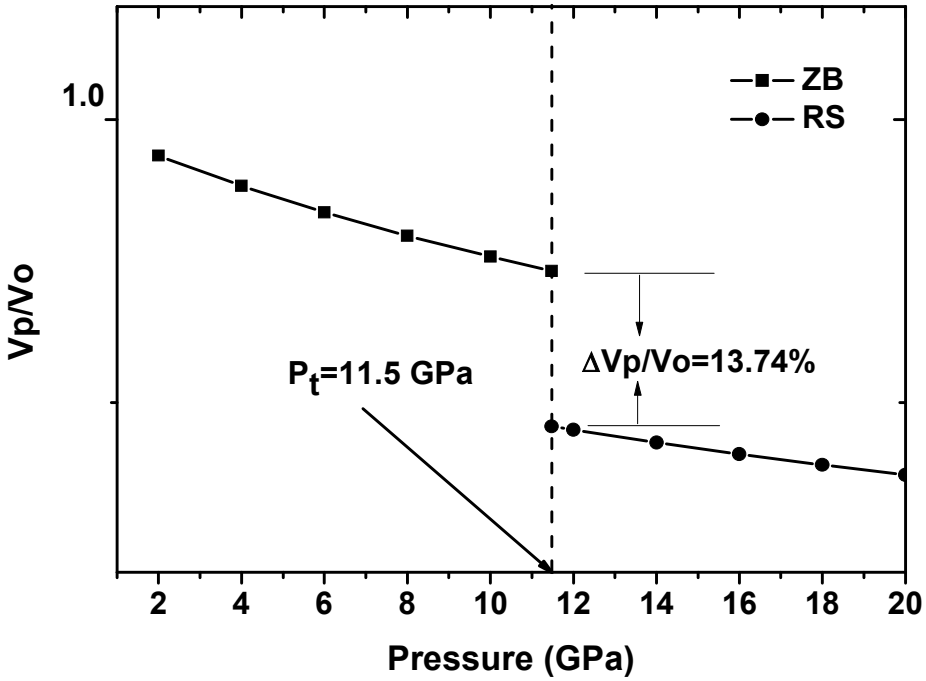

Figure 5.9. Normalized volume as a function of pressure of ZnSe-ZB and ZnSe-RS

5.3. ELASTIC PROPERTIES

(a) Zinc Sulfide (ZnS)

In the present study of Zinc Sulfide (ZnS), the elastic constants are calculated within the GGA only as it has already been shown in previous calculations that the structural phase transition within the GGA gives us better results than LDA. The structural phase transition of ZnS from the zincblende to rocksalt structure with the GGA method has been calculated in figure 5.2 which is occurred at 17.6 GPa pressure. Therefore the elastic constants for ZnS-ZB are calculated corresponding to pressure ranging from 0 GPa to 16 GPa pressure and from 18 GPa to 30 GPa pressure for ZnS-RS. The values of elastic constants of the present work satisfy the mechanical stability conditions: $(C_{11}+2C_{12}) > 0$; $C_{11}-C_{12} > 0$; $C_{44} > 0$; $C_{11} > 0$ for the both the phases.The figure 5.10 shows the variation of elastic constants with pressure. There is a linear variation of elastic constants with pressure up to 16GPa of the ZB phase and 18GPa to 30 GPa of RS phase after the transition pressure of 17.6 GPa.

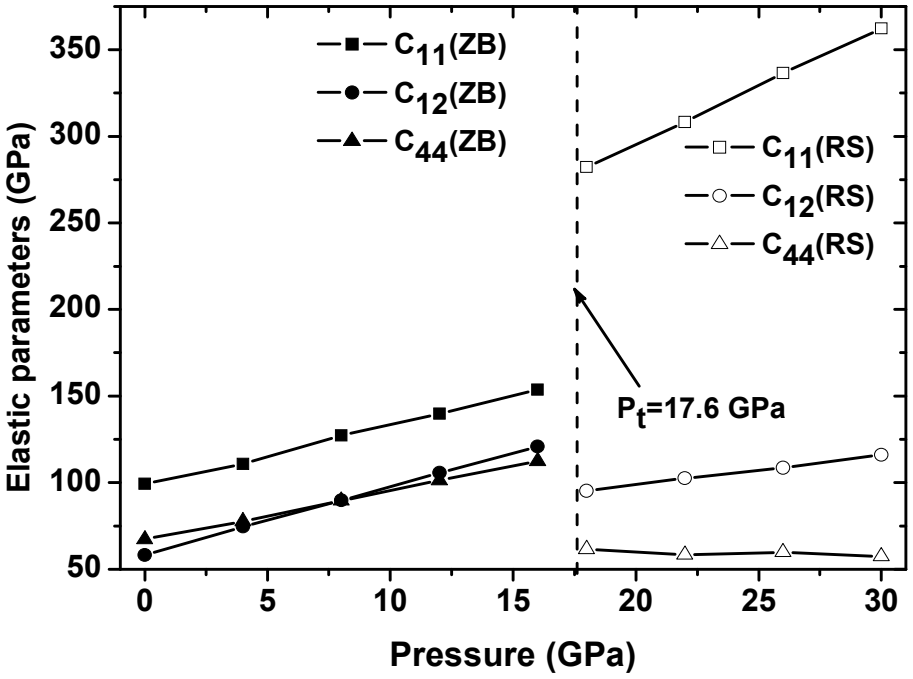

Figure 5.10. Elastic constants (C_{11}, C_{12}, C_{44}) as a function of pressure for ZnS-ZB and ZnS-RS structure

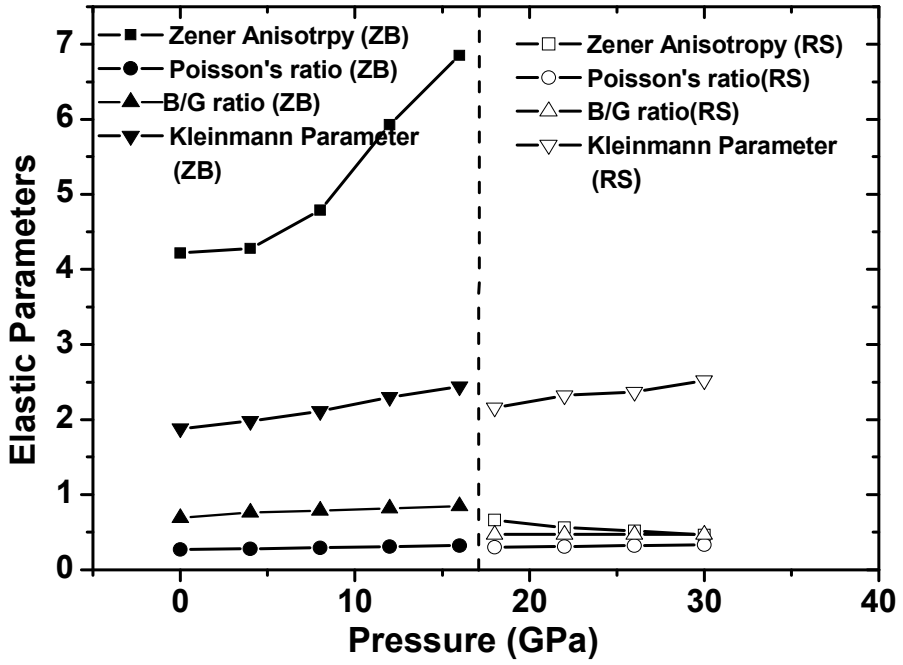

Figure 5.11. Elastic parameters (Zener Anisotropy factor, Poisson's ratio, Kleinmann parameter and B/G ratio) as a function of pressure for ZB and RS phase of ZnS

In the light of these observations, the elastic parameters such as Zener Anisotropy factor (A), Poisson's ratio (υ), Kleinmann's parameter (ζ), B/G ratio, Young's modulus (Y) and Deby's temperature (θ_D) are calculated for both ZnS-ZB and ZnS-RS phases at different pressures as shown in figure 5.11. These elastic parameters are used to determine the mechanical and thermal behavior of ZnS at high pressures.

In figure 5.11, a consistent pattern of linear variation in the elastic parameters with increase in pressure is observed. The Zener Anisotropy factor (A) shows a variation from 4.22 to 6.85 in the ZB phase while it decreases from 0.66 to 0.46 with pressure in case of RS phase. In the present study, the Kleinmann parameter (ζ) of the ZB phase is found to vary from 0.69 to 0.85 with pressure showing bond stretching in the ZB phase while it is found to be 0.48 to 0.46 showing shrinkage in bond bending in the RS phase. The B/G ratio of ZnS-ZB phase increases from 1.88 to 2.44 while the ZnS-RS phase shows an increase from 2.16 to 2.52. Hence we conclude that the brittle nature of the ZB phase of ZnS becomes ductile as the pressure increases and retains its ductility even after it undergoes a structural phase transition to RS phase.

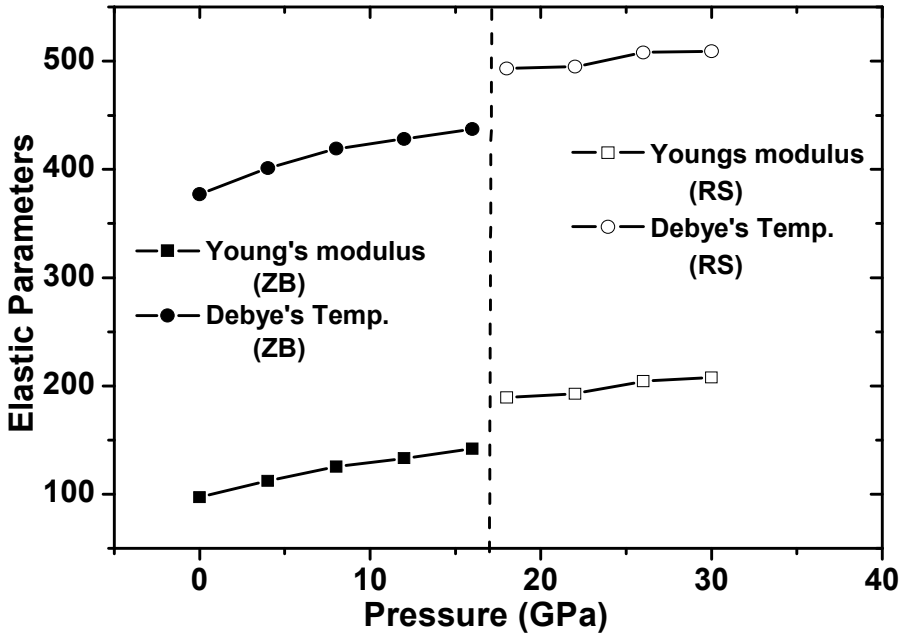

Figure 5.12. Elastic parameters (Young's modulus and Debye's temperature) as a function of pressure of ZnS in ZB phase and RS phase

The elastic parameters (Young's modulus and Debye's temperature) as a function of pressure for both ZnS-ZB and ZnS-RS phases are shown in figure 5.12. From the figure it is seen that with increase in pressure the value of Y increases from 97.18 GPa to 142.08 GPa in the ZB phase while in case of RS phase the value of Y increases from 189.43 GPa to 207.86 GPa. Thus ZnS becomes more rigid with increase in pressure in both the ZB phase and RS phase. As the pressure increases, the value of Debye's temperature also increases from 377 K to 438 K for the ZB phase and from 493 K to 509 K for the RS phase indicating stiffer lattice and better thermal conductivity in both the phases.

(c) Cadmium Telluride (CdTe)

In this sub section, the elastic constants of Cadmium Telluride (CdTe) are calculated at various pressure ranging from 0 GPa to 3 GPa pressure of CdTe-ZB and from 5 GPa to 7 GPa pressure of CdTe-RS as the structural phase transition from ZB to RS occurred at 4 GPa pressure as shown above. The present results are found to satisfy the mechanical stability conditions for both

the phases and shown in figure 5.13. It is observed that under pressure there is a linear variation in the elastic constants up to 2 GPa pressure in ZB phase and 5 GPa to 7 GPa pressure in the RS phase. Around 3 GPa pressure, the stability condition of CdTe-ZB phase is not satisfied indicating that the structural transformation from ZB to RS starts at around 3 GPa pressure and completes at 4 GPa pressure. The elastic parameters like Zener anisotropic factor (A), Poisson's ratio (υ), Kleinmann parameter (ζ), B/G ratio, Young's modulus (Y), and Debye's temperature (θ_D) to determine the mechanical and thermal behaviour of both the phases as shown in figure 5.14.

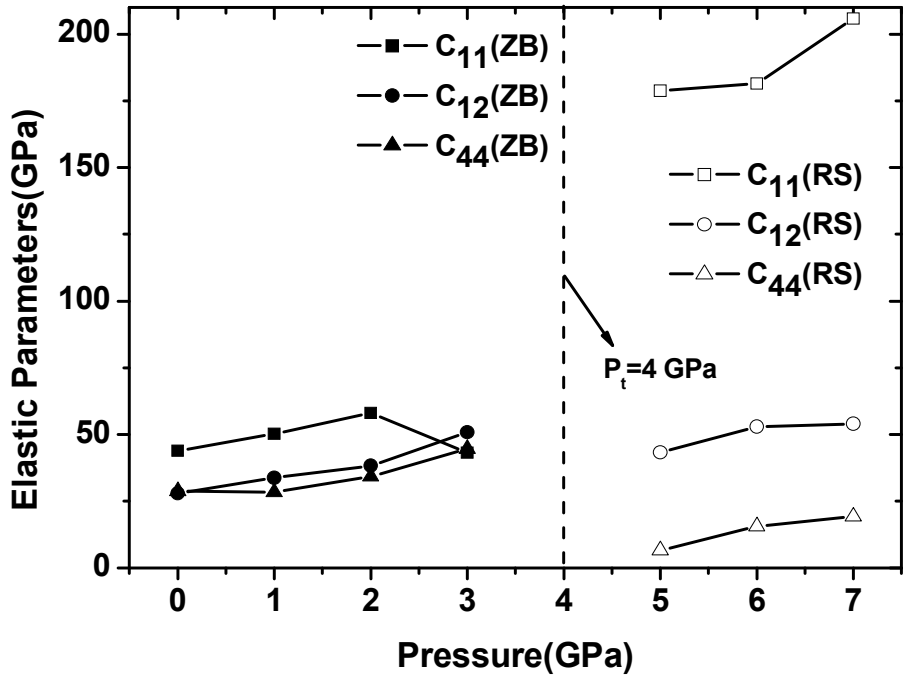

Figure 5.13. Elastic parameters versus pressure for ZB and RS phase of CdTe

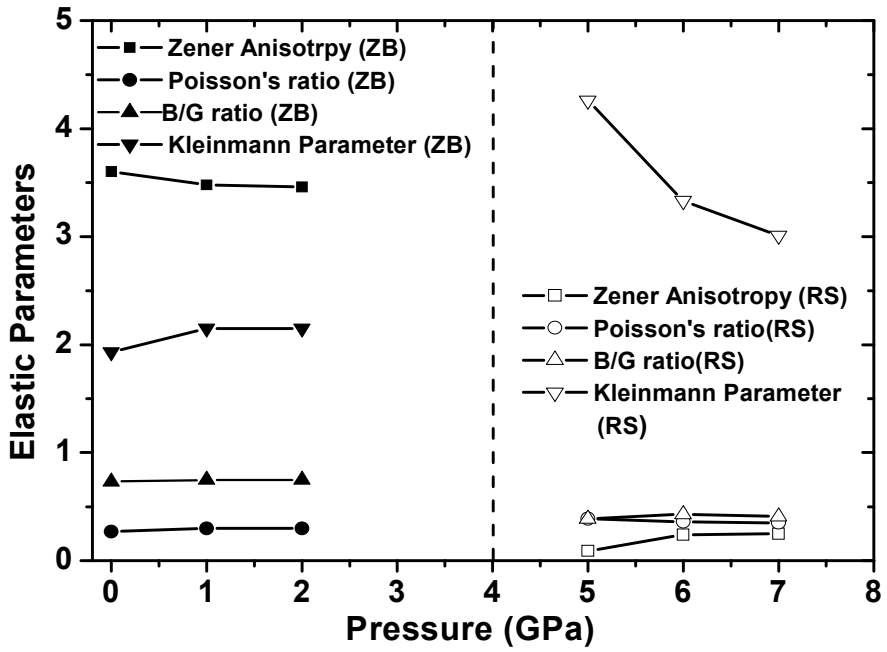

Figure 5.14. Elastic parameters (Zener Anisotropy factor, Poisson's ratio, Kleinmann parameter and B/G ratio) as a function of pressure for ZB and RS phases of CdTe

As the pressure increases, the Zener Anisotropy factor (A) for CdTe-ZB phase decreases from 3.60 to 3.46 while for CdTe-RS, it increases from 0.09 to 0.25 indicating that CdTe is not an elastically isotropic material. There is increase in Poisson's ratio (υ) from 0.27 to 0.30 in the ZB phase and decrease from 0.39 to 0.35 in the RS phase indicating higher ionic contribution in intra-atomic bonding with increasing pressure in both the phases. The present result also indicates that inter atomic forces tends to be more central with pressure. As the pressure increases, Kleinmann parameter does not vary much and remains around 0.75 for CdTe-ZB and 0.41 for CdTe-RS indicating shrinkage in bond-stretching in both phases. The B/G ratio for CdTe-ZB ranges from 1.93 to 2.15 with increase in pressure indicating ductile nature at high pressure. For CdTe-RS, B/G ratio decreases from 4.26 to 3.01 with increase in pressure but is greater than 1.75. Hence we can conclude that both CdTe-ZB and CdTe-RS retains its ductile nature even at higher pressures.

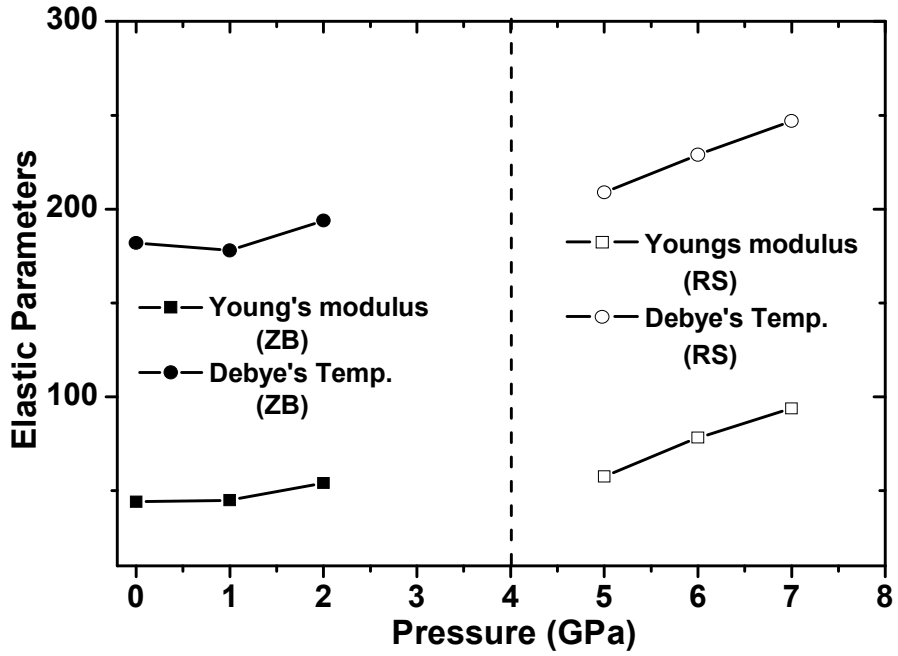

Figure 5.15. Elastic parameters (Young's modulus and Debye's temperature) as a function of pressure of CdTe in ZB phase and RS phase

In figure 5.15, the elastic parameters (Young's modulus and Debye's temperature) as a function of pressure for both CdTe-ZB and CdTe-RS phases are shown. With increase in pressure the value of Y increases from 44.08 GPa to 54.15 GPa in CdTe-ZB while in CdTe-RS it increases from 57.65 GPa to 93.84 GPa. Hence CdTe becomes stiffer with increase in pressure in both phases. The Debye's temperature calculated also shows an increase from 181 K to 194 K for CdTe-ZB and from 209 K to 247 K in CdTe-RS phase indicating better thermal conductivity under pressure.

c) Zinc Selenide (ZnSe)

As mentioned above, phase transition of Zinc Selenide (ZnSe) under pressure occurs at 11.5 GPa and thus figure 5.16 shows the elastic constants of ZnSe-ZB structure at various pressure from 0 GPa to 8 GPa pressure and from 12 GPa to 18 GPa pressure in rocksalt structure and found to satisfy the mechanical stability conditions for both phases.

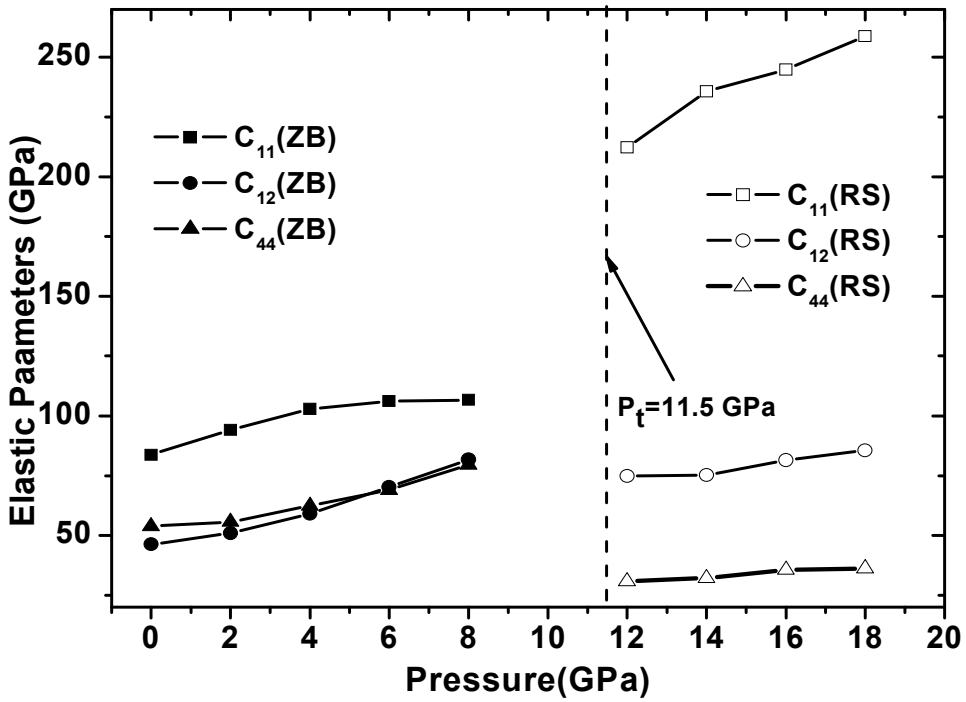

Figure 5.16. Elastic constants (C_{11}, C_{12}, C_{44}) as a function of pressure of ZnSe-ZB and ZnSe-RS phase

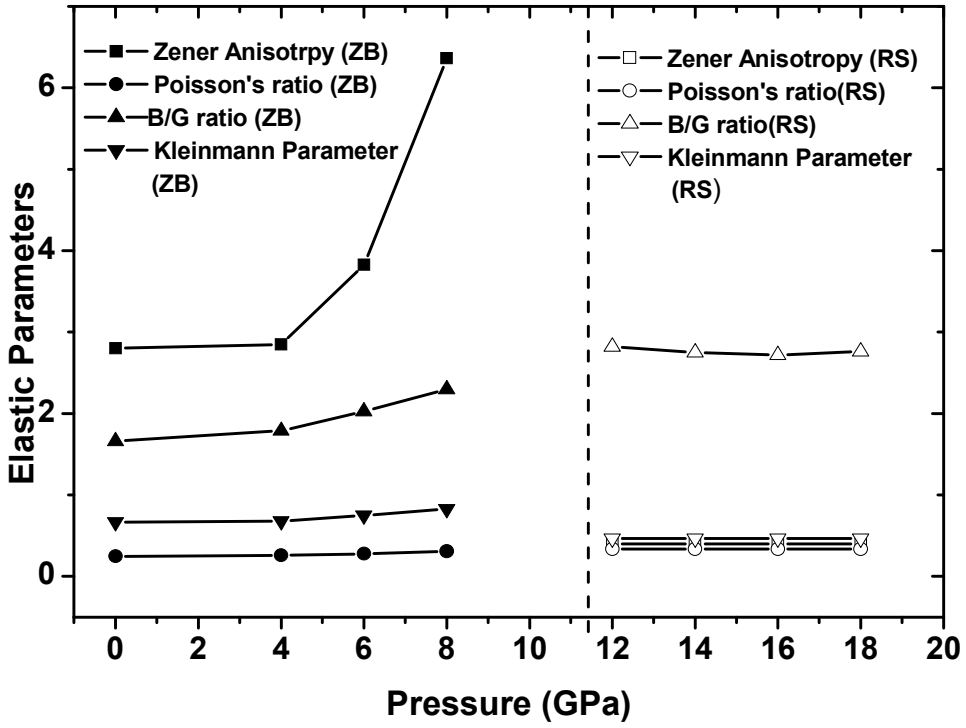

Figure 5.17. Elastic parameters (Zener Anisotropy factor, Poisson's ratio, Kleinmann parameter and B/G ratio) as a function of pressure for ZnSe-ZB and ZnSe-RS

In figure 5.17 our calculated elastic parameters (Zener Anisotropy factor (A), Poisson's ratio (υ), kleinmann's parameter (ζ) and B/G ratio) as a function of pressure are shown.

The Zener Anisotropy factor, A shows a variation from 2.88 to 6.36 in the ZB phase while in the RS phase it decreases from 0.44 to 0.41with increasing pressure. The value of Poisson's ratio, υ increases from 0.25 to 0.35 in ZB phase indicating higher ionic contribution in the inter atomic bonding with increasing pressure while in the RS phase it remains around 0.34. In the present study, the Kleinmann parameter,ζ is found to vary from 0.67 to 0.83 with pressure of the ZB phase while it is found to decrease from 0.49 to 0.47 in the RS phase showing shrinkage in bond stretching in the ZB phase and shrinkage in bond bending in the RS phase. With increasing pressure, the B/G ratio of ZnSe-ZB phase increases from 1.66 to 2.30 while ZnSe-RS phase shows a decrease from 2.82 to 2.76. Hence the ZB phase is brittle in nature but as the pressure increases it tends to becomes ductile and retains its ductility even after it undergoes a structural phase transition to RS phase.

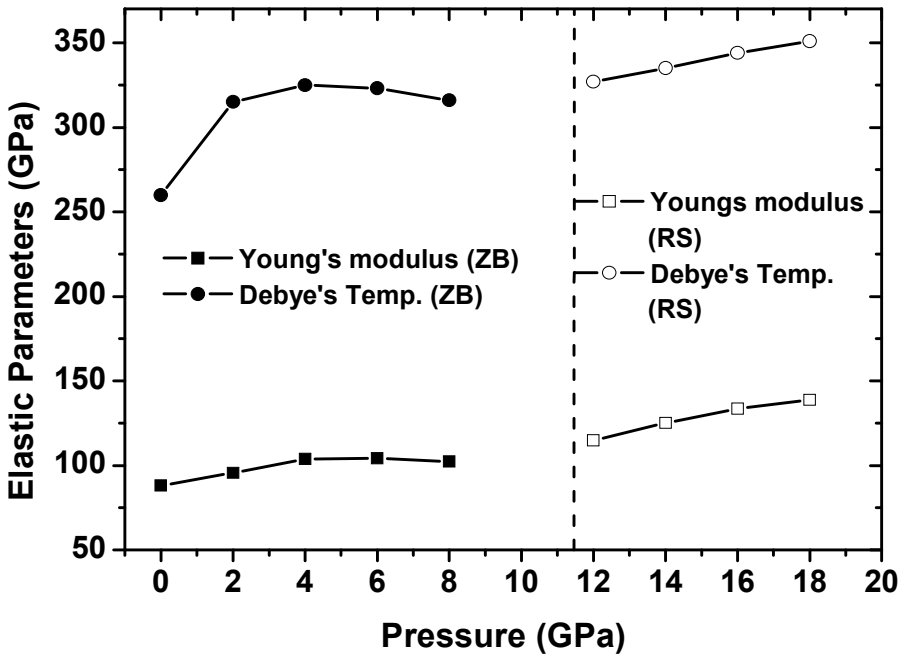

Figure 5.18. Elastic parameters (Young's modulus and Debye's temperature) as a function of pressure of ZnSe in ZB phase and RS phase

The elastic parameters (Young's modulus and Debye's temperature) as a function of pressure for both ZnSe-ZB and ZnSe-RS phases are shown in figure 5.18. The value of Y increases from 88.09 GPa to 102 GPa in the ZB phase while in the RS phase the value of Y increases at first from 114.78 GPa to 104.24 GPa and then decreases to 102.32 GPa as it comes nearer to the transition pressure. Thus ZnSe-ZB becomes more rigid with increase in pressure but certain deformation is found to occur just before it undergoes a structural transformation to the RS phase and after completion of the transition it attains its rigidity again as pressure goes on increasing. Similarly the value of Debye's temperature also increases from 260 K to 323 K for the ZB phase indicating stiffer lattice and better thermal conductivity but slightly decreases just before it undergoes structural transformation to the RS phase and after transition to the RS phase it again increase from 327K to 351 K showing better thermal conductivity.

5.4. ELECTRONIC PROPERTIES

(a) Zinc Sulfide (ZnS)

The electronic band structure calculation of ZnS-ZB and ZnS-RS at 0 GPa pressure are performed within (a) LDA, (b) GGA and (c) mBJ-GGA methods and are shown in figure 5.19 and figure 5.20 respectively. For ZnS-ZB, figure 5.1 (a, b and c) shows that the valance band maximum and conduction band minimum occurs at the Γ point confirming a direct band gap. The band gap with LDA and GGA calculation shows a band gap of 1.89 eV and 1.99 eV respectively while with mBJ-GGA calculation gives a band gap of 3.5 eV which is very close to the experimental values of 3.6 eV [101]. Again the band structures of ZnS-RS are shown in figure 5.20 (a, b and c). In figure 5.20 (a) and 5.20 (b) with the LDA and GGA calculation, there is a crossing over of the conduction band at the Fermi energy towards the valance band. However electronic band structure calculation with the mBJ-GGA as shown in figure 5.20 (c) shows that the valance band maximum occurs at the Γ point while the conduction band minimum occurs at L point confirming an indirect band gap.

Thus the implementation of the mBJ-GGA potential resolves the underestimation of the band gaps.

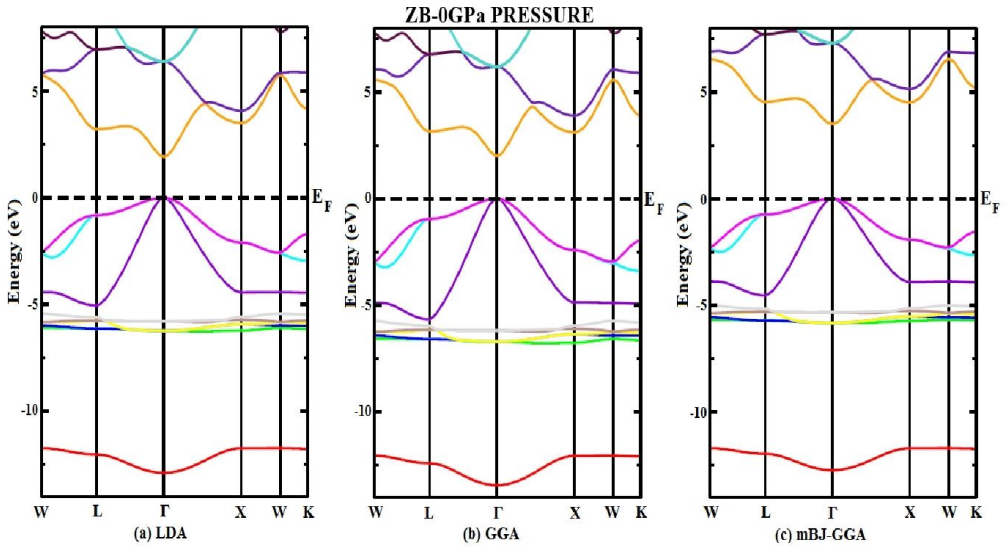

Figure 5.19. Band structure of ZnS-ZB at 0 GPa pressure within (a) LDA, (b) GGA and (c) mBJ-GGA

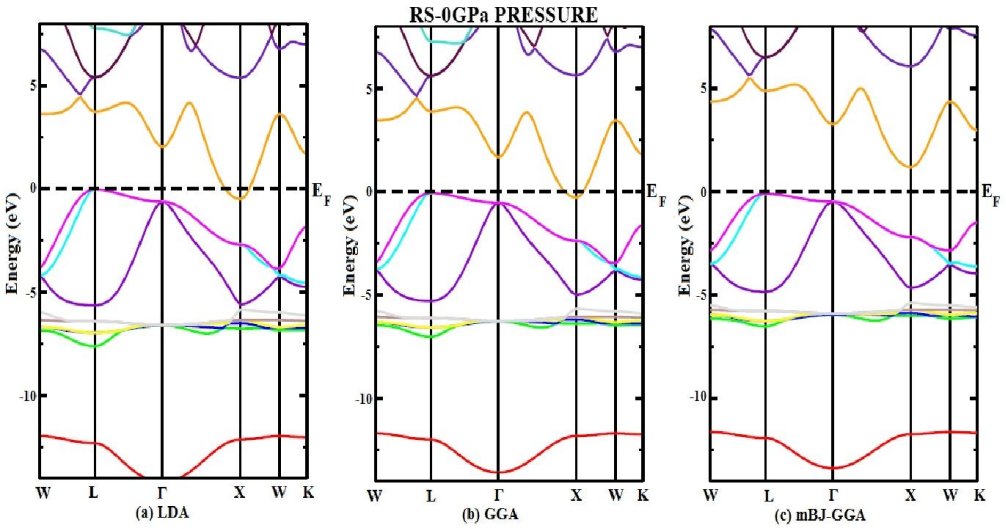

Figure 5.20. Band structure of ZnS-RS at 0 GPa pressure within (a) LDA, (b) GGA and (c) mBJ-GGA

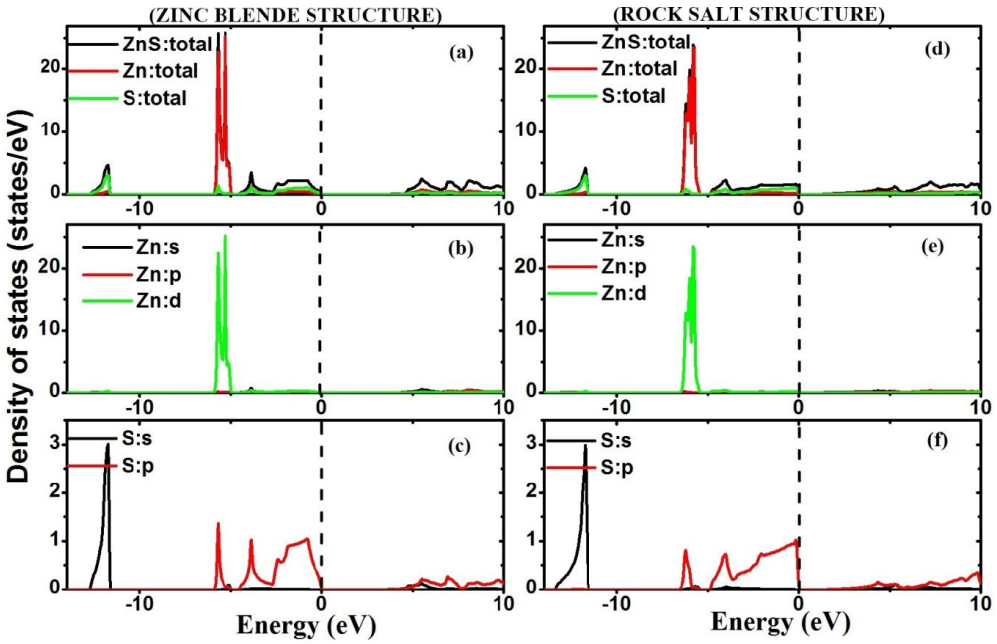

Figure 5.21. Total and Partial DOS of ZnS-ZB and ZnS-RS within mBJ-GGA.

The origin of the energy band structure of a compound is related to the corresponding density of states. Therefore for better understanding of band gaps the total and partial density of states (DOS) are studied. But since we find that calculations within the mBJ-GGA gives us better results than within LDA and GGA, we have therefore studied the total DOS and partial DOS within the mBJ-GGA only. In figure 5.21, the total and partial DOS of ZnS-ZB and ZnS-RS are shown. From figure 5.21(a), (b) and (c), for ZnS-ZB phase, we find that the lowest band appearing in energy band diagram is mainly contributed from s-non metal (S atom) orbital while the valance band is mainly contributed by the d-metal (Zn- atom) orbital. Again from figure 5.21(d), (e) and (f) for ZnS-RS, the lowest band is mainly contributed by the s-non metal (S atom) orbital while the valance band is mainly contributed by the d-metal (Zn-atom) orbital with little contribution from the p (S-atom) orbital.

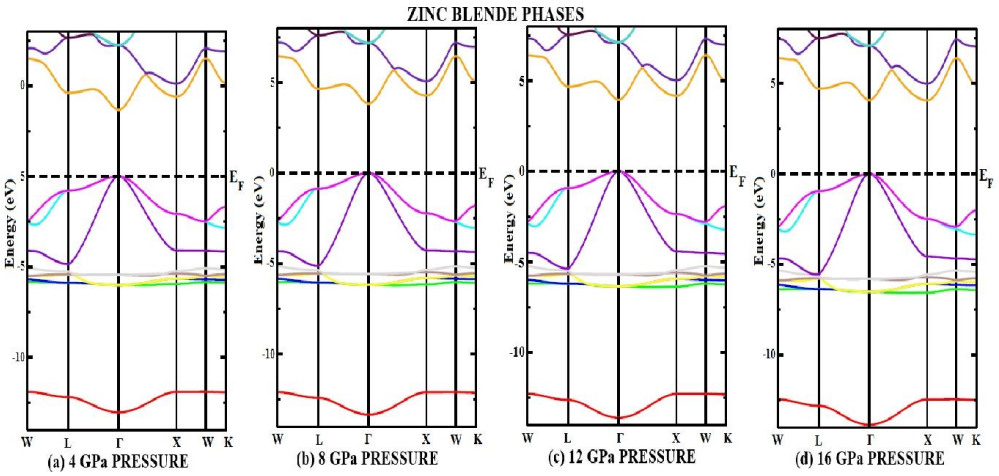

Figure 5.22. Energy band diagram ZnS-ZB at (a) 4 GPa pressure (b) 8 GPa pressure (c) 12 GPa pressure and (d) 16 GPa pressure.

Next we are interested to study the variation of band diagram with pressure. Figure 5.22 (a, b, c) and d) shows the energy band diagram of ZnS-ZB structure at different pressures. we observe from the band structure diagrams (in figure 5.22) that as the pressure increases to 5 GPa, 10 GPa 15 GPa and 20 GPa, there is an increase in the gap between Γ-L point while the gap between Γ-X decreases towards the Fermi level indicating possibilities of crossing over of the conduction band towards the valance band at higher pressure indicating to be metallic nature of ZnS-RS. The variation in the energy band gap with pressure for ZnS-ZB is also shown in figure 5.23 for clear analysis of the changes in the gap between Γ- Γ point, Γ-X point and Γ-L point with pressure.

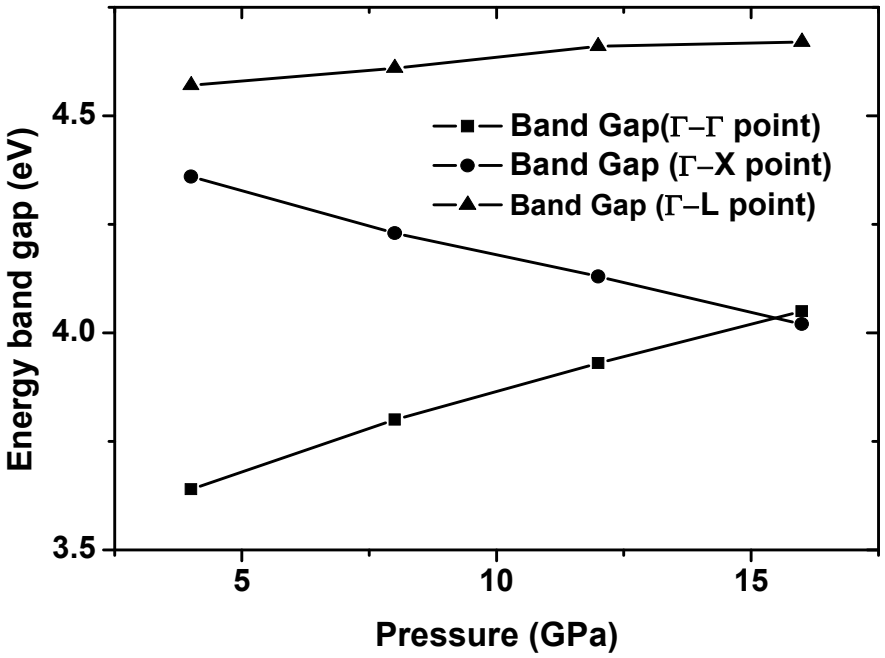

Figure 5.23. Variation in Energy band gaps of ZnS-ZB phase with pressure.

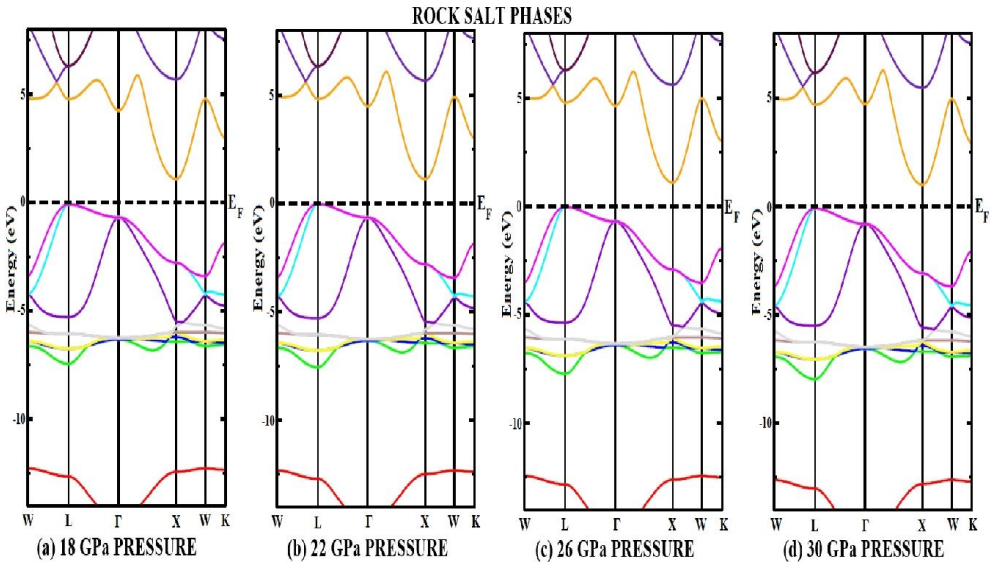

Figure 5.24. Energy band diagram ZnS-RS phase at (a) 18 GPa pressure (b) 22 GPa pressure (c) 26 GPa pressure and (d) 30 GPa pressure

In figure 5.24(a, b, c and d) the energy band diagrams of ZnS-RS phase at different pressures are given. From the figure we find that the indirect band gap nature of ZnS-RS is retained even at high pressure without much variation. Hence we conclude that the energy band gap of ZnS-ZB phase is

affected by pressure while the energy band gap of ZnS-RS phase is not much affected by pressure.

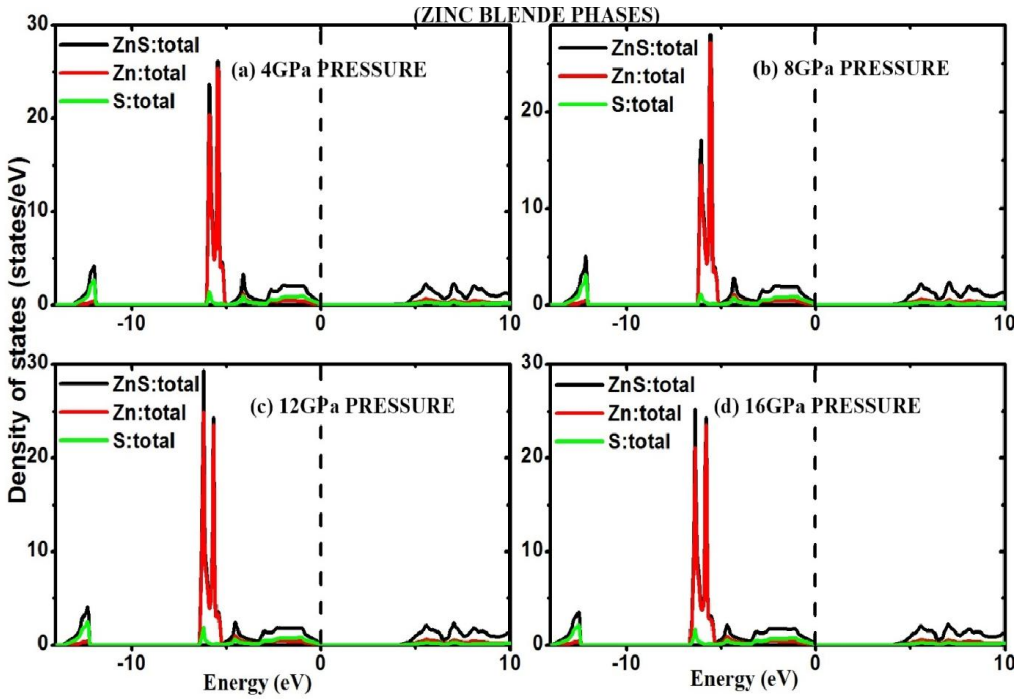

Figure 5.25. Total DOS of ZnS-ZB structure at (a) 4 GPa pressure (b) 8 GPa pressure (c) 12 GPa pressure and (d) 16 GPa pressure.

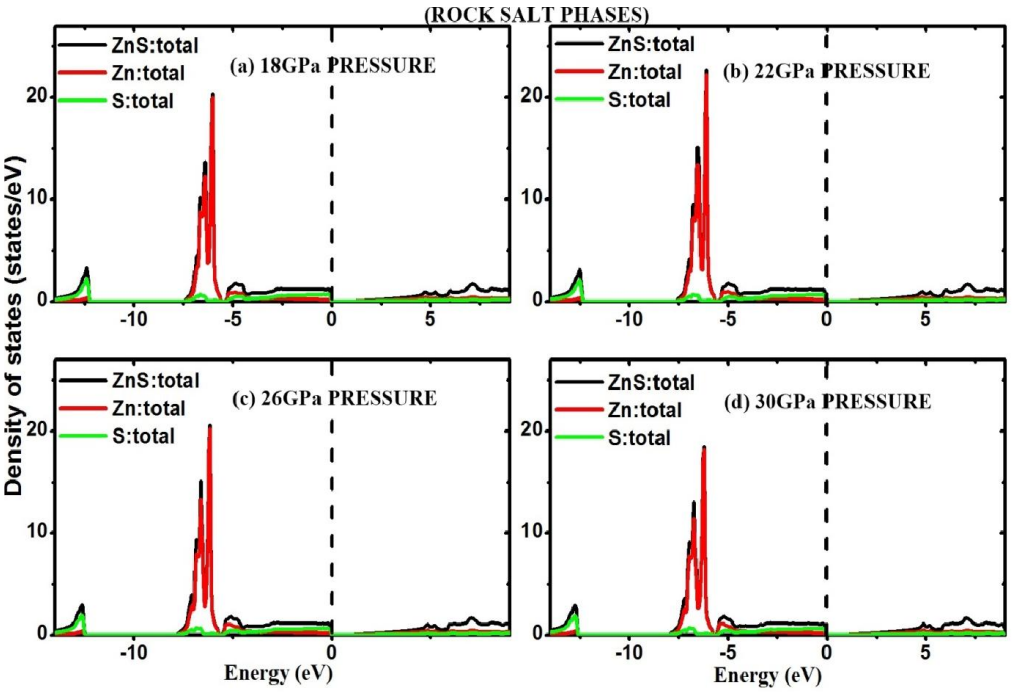

Figure 5.26. Total DOS of ZnS-RS structure at (a) 18 GPa pressure (b) 22 GPa pressure (c) 26 GPa pressure and (d) 30 GPa pressure

Further, the total DOS of ZnS-ZB at (a) 4 GPa pressure (b) 8 GPa pressure (c) 12 GPa pressure and (d) 16 GPa pressure are given in figure 5.25. From the figure we find that in the lowest band the contribution of the S atom merely increases with increase in pressure while the contribution of the Zn atom decreases with increasing pressure. Again in the valance band as the pressure increases the contribution of Zn atom increases up to 12 GPa and its contribution starts to decrease at 16 GPa which is expected near to phase transition pressure (around17GPa) while there is no change in the contribution of S atom. In figure 5.26, the total DOS of ZnS-RS at (a) 18 GPa pressure (b) 22 GPa pressure (c) 26 GPa pressure and (d) 30 GPa pressure are shown. From the figure we see that in the lowest band, with increase in pressure, the contribution of the S atom does not change. In the valance band, the contribution of the Zn-atom increases and then decreases as the pressure goes on increasing. Hence for ZnS-ZB phase the change in pressure affects both the Zn atom as well as the S atom but in case of ZnS-RS phase the change in pressure mainly affects the Zn atom.

(b) Cadmium Telluride (CdTe):

Figure 5.27(a, b and c) and 5.28(a, b and c) show the electronic band structure of CdTe-ZB and CdTe-RS at zero pressure within (a) LDA, (b) GGA and (c) mBJ-GGA methods. Energy band diagrams in figure 5.27 (c) of CdTe-ZB reveals a direct band gap of 1.46 eV with mBJ-GGA which is close to the experimental values of 1.44eV [101]. In figures 5.28 (a), (b) and (c), there is crossing over of the conduction band at the Fermi energy towards the valance band indicating metallic nature of CdTe-RS.

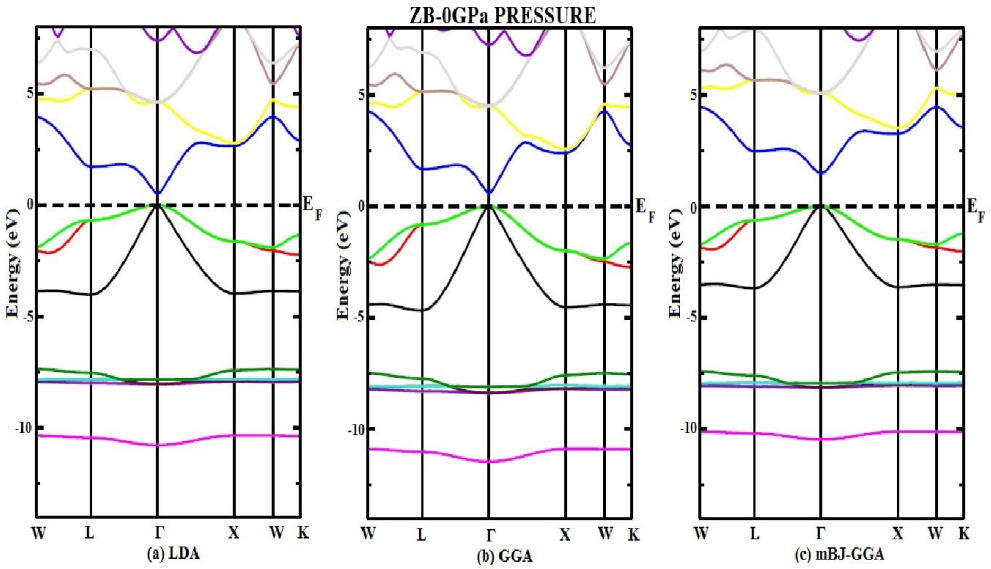

Figure 5.27. Band structure of CdTe-ZB at 0 GPa pressure within (a) LDA, (b) GGA and (c) mBJ-GGA methods

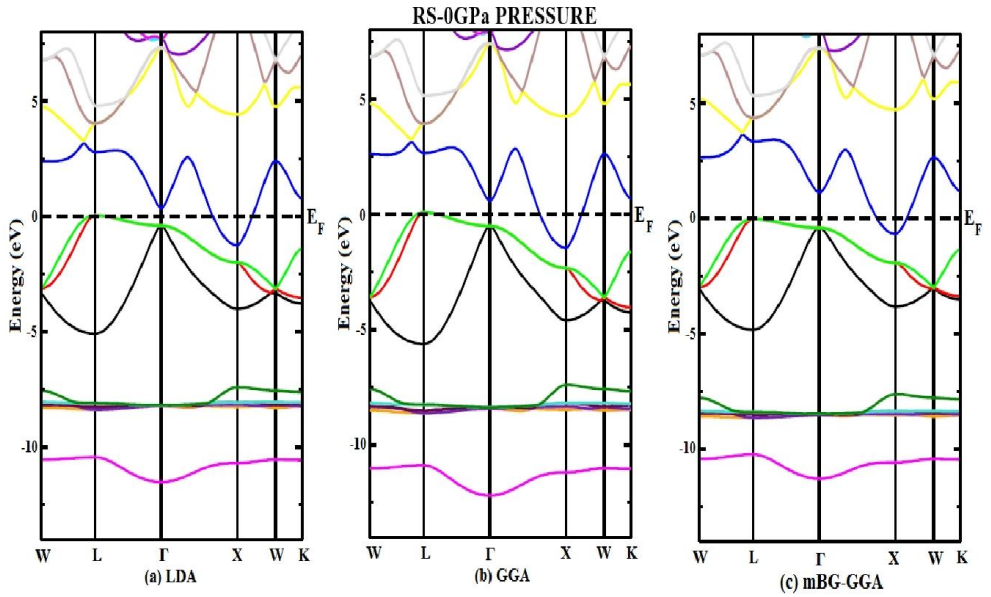

Figure 5.28. Band structure of CdTe-RS at 0 GPa pressure within (a) LDA, (b) GGA and (c) mBJ-GGA methods

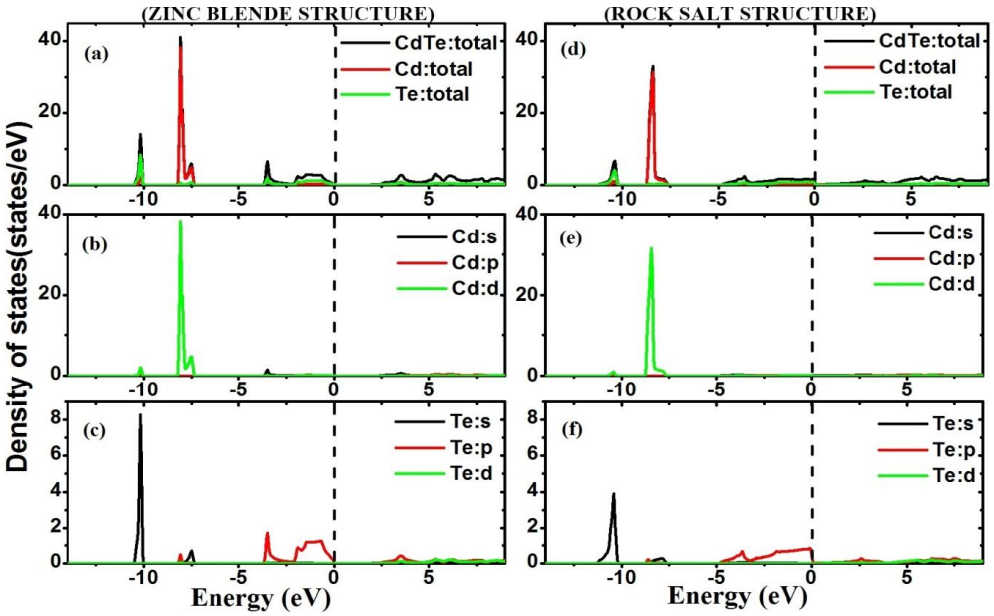

Figure 5.29. Total and Partial DOS of CdTe-ZB and CdTe-RS within mBJ-GGA method

From the DOS plot of CdTe-ZB in figure 5.29(a, b and c) it is observed that first lowest band in the band structure is mainly contributed by the s-non metal (Te-atom) orbital with little contribution from the d-metal (Cd-atom) orbital while the second lowest band shows higher contribution of the d-metal (Cd atom) orbital. The valance band is mainly contributed by the s-metal (Cd-atom) orbital and s-non metal (Te-atom) orbital. Also in figure 5.29(d, e and f) of CdTe-RS, the lowest band is mainly contributed by the s-non metal (Te atom) orbital with little contribution from the p-metal (Cd-atom) orbital and d-metal (Cd-atom) orbital while the valance band is mainly contributed by the d-metal (Cd-atom) orbital with little contribution from the p-non metal (Te-atom) orbital.

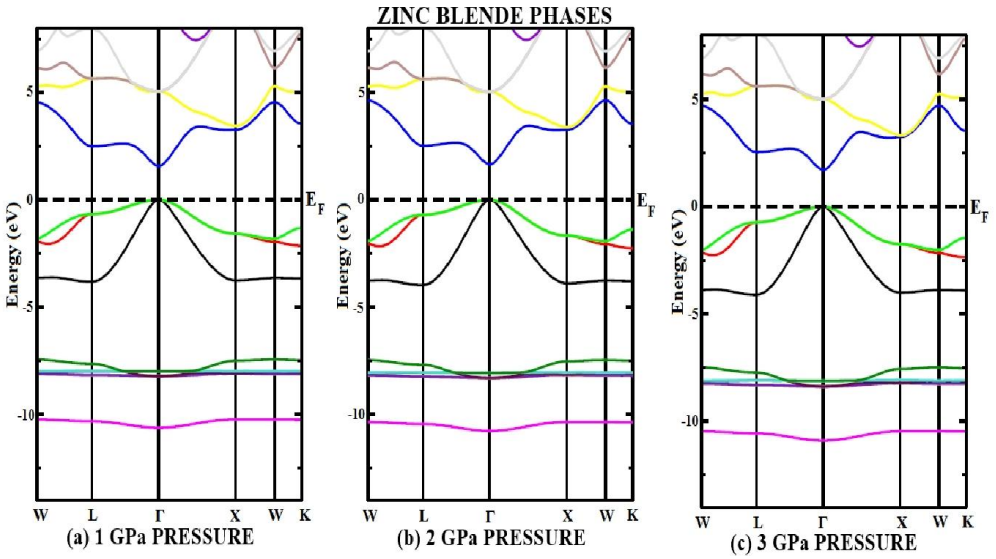

Figure 5.30. Energy band diagram CdTe-ZB at (a) 1 GPa pressure (b) 2 GPa pressure and (c) 3 GPa pressure.

Figure 5.31(a, b, c and d) shows the energy band diagrams of CdTe-ZB phase at different pressures. In figure 5.31, as the pressure increases to 1 GPa, 2 GPa and 3 GPa pressure, the gap between the Γ- Γ point increases. The variations of gaps at Γ- Γ point, Γ-L point and Γ- X point with increase in pressure are given in figure 5.31. Also Figure 5.32 (a, b and c) shows energy band diagrams of CdTe-RS phase at different pressures showing metallic nature is retained even at high pressure without much variation.

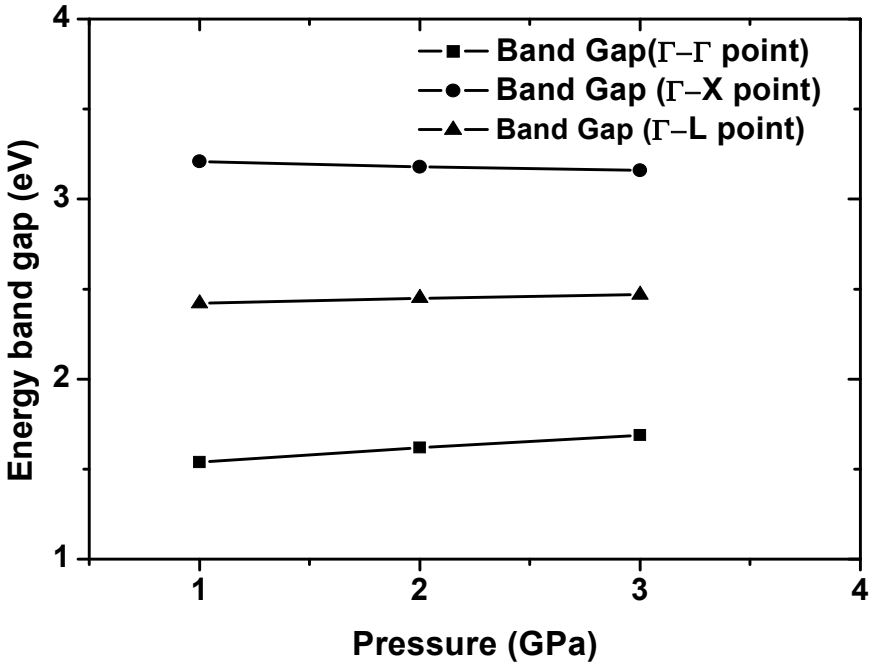

Figure 5.31. Variation of Energy band gaps of CdTe-ZB phase with pressure

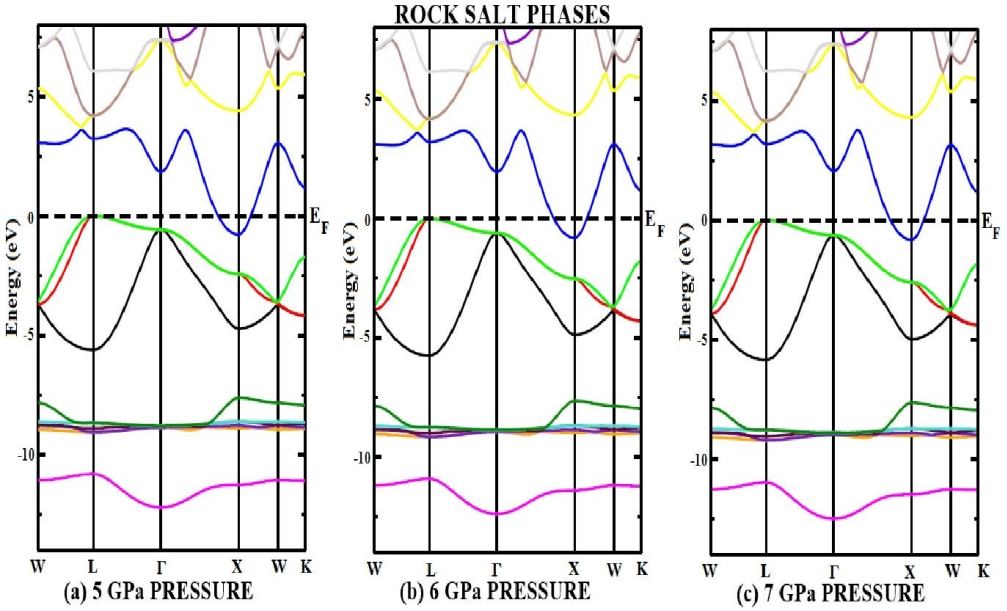

Figure 5.32. Energy band diagram CdTe-RS at (a) 5 GPa pressure (b) 6 GPa pressure and (c) 7 GPa pressure

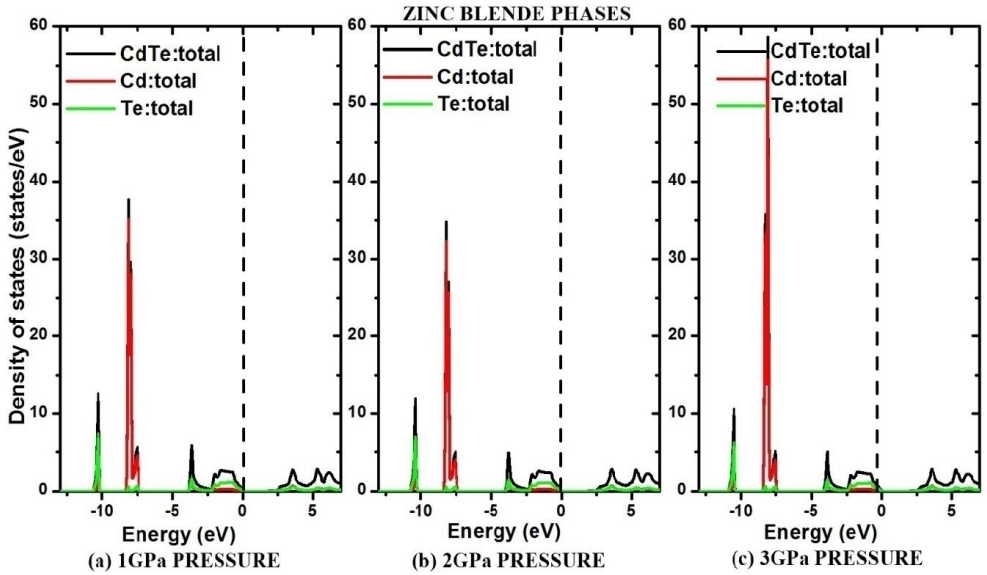

Figure 5.33. Total DOS of CdTe-ZB structure at (a) 1 GPa pressure, (b) 2 GPa pressure and (c) 3 GPa pressure

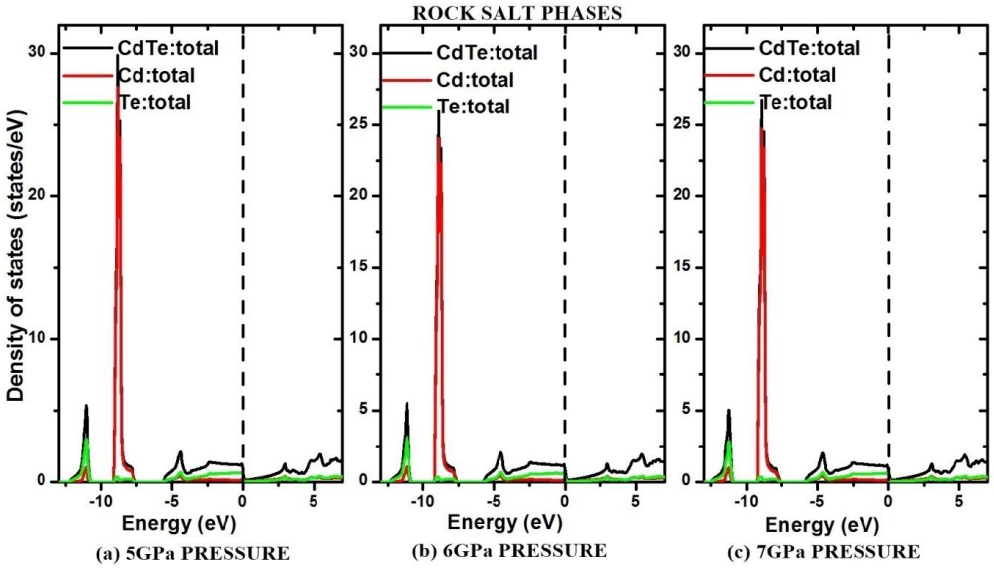

Figure 5.34. Total DOS of CdTe-RS structure at (a) 5 GPa pressure, (b) 6 GPa pressure and (c) 7 GPa pressure

The total DOS of CdTe-ZB at (a) 1 GPa pressure (b) 2 GPa pressure and (c) 3 GPa pressure are given in figure 5.33. The variation of gap between valence and conduction band observed in the DOS plot clearly reflects the increase of band gap with pressure in the band diagram as discussed above. Also figure 5.34 shows the total DOS of CdTe-RS at (a) 5 GPa pressure (b) 6 GPa pressure and (c) 7 GPa pressure. In this plot, it is clearly observed the crossing

of orbitals towards valence and conduction band around Fermi line. It confirms the metallic nature of CdTe-RS structure as observed in band diagram as mentioned above.

(c) Zinc Selenide (ZnSe)

In the same way as discussed, the electronic band structure of ZnSe in zincblende and rocksalt structure at 0 GPa pressure calculated with the three methods (LDA, GGA, mBJ-GGA) are shown in figure 5.35 and figure 5.36. Figure 5.35 (c) shows ZnSe-ZB is a direct band gap compound semiconductor of 1.46eV. As we see crossing over of orbital in figure 5.36 at the Fermi line indicates metallic nature of ZnSe-RS.

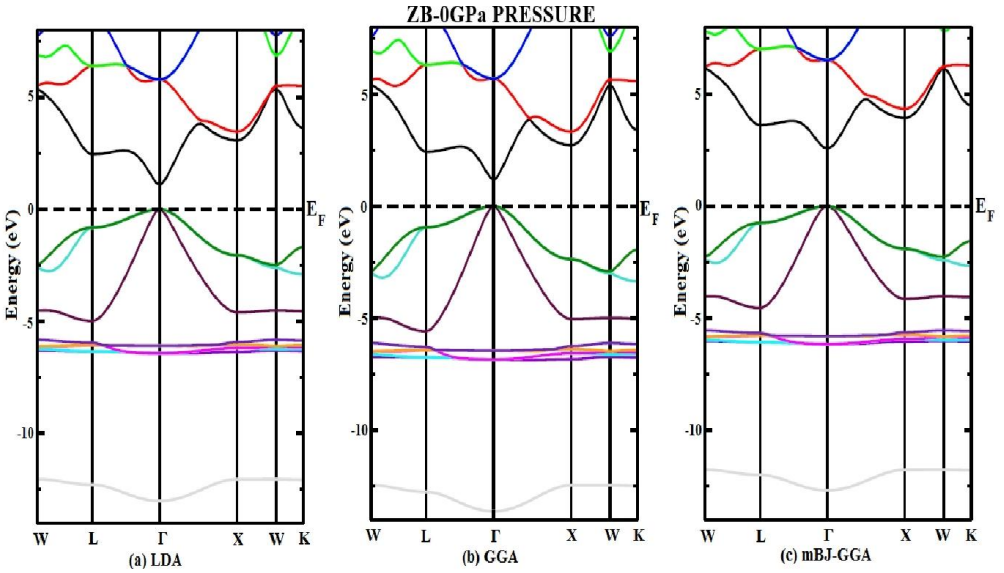

Figure 5.35. Band structure of ZnSe-ZB at 0 GPa pressure within (a) LDA, (b) GGA and (c) mBJ-GGA

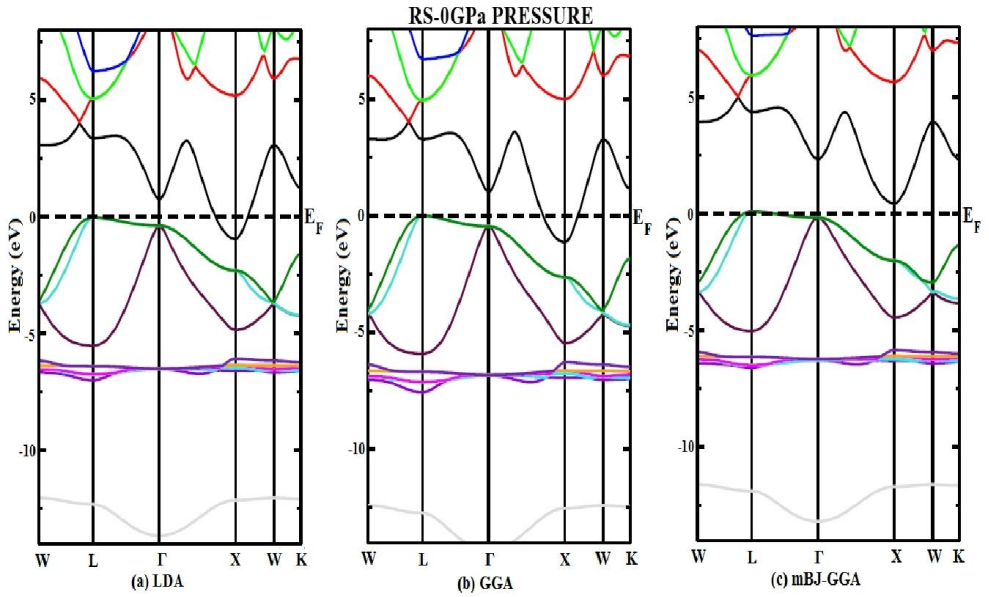

Figure 5.36. Band structure of ZnSe-RS at 0 GPa pressure within (a) LDA, (b) GGA and (c) mBJ-GGA

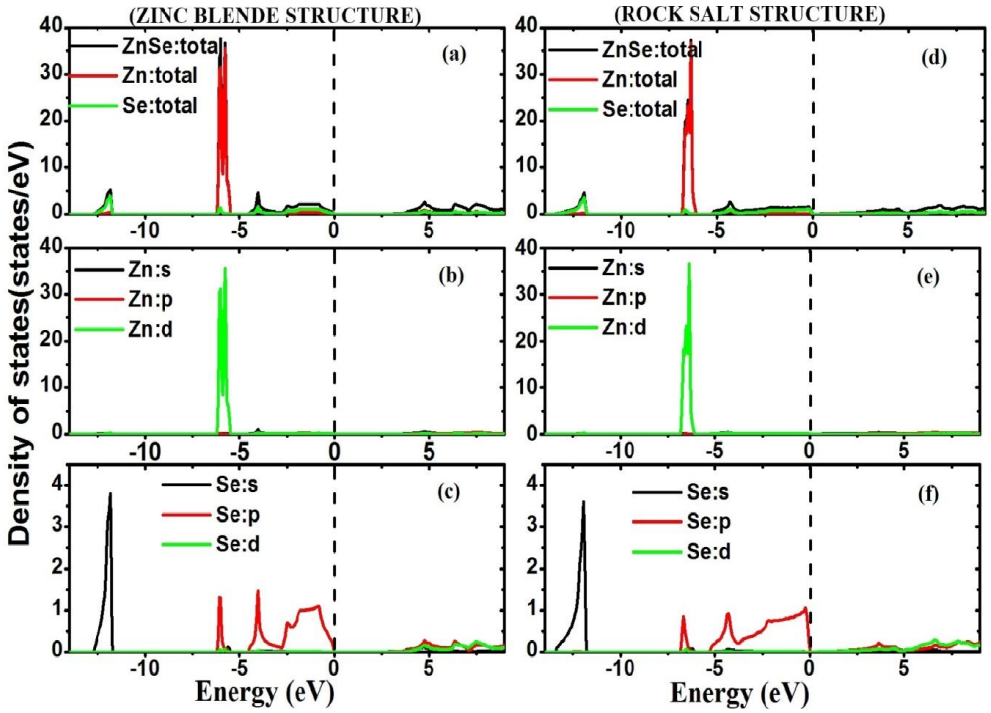

Figure 5.37. Total and Partial DOS of ZnSe-ZB and ZnSe-RS within mBJ-GGA

The total and partial DOS of ZnSe for both the phases within mBJ-GGA are shown in figure 5.37 (a-f). For the ZB phase, in figure 5.37(a), (b) and (c), we see that the lowest band is mainly contributed from s-non metal (Se atom) orbital with little contribution from the p-metal (Zn atom) orbital and d-metal (Zn atom) orbital while the valance band is mainly contributed by the d-metal

(Zn atom) orbital along with little contribution from the p-non metal (Se-atom) orbital. Again from figure 5.37(d), (e) and (f) for RS phase we find that the lowest band is mainly contributed by the s-non metal (Se atom) orbital while the valance band is mainly contributed by the d-metal (Zn-atom) and a small contribution from p-metal orbital with p-non metal (Se-atom) orbital.

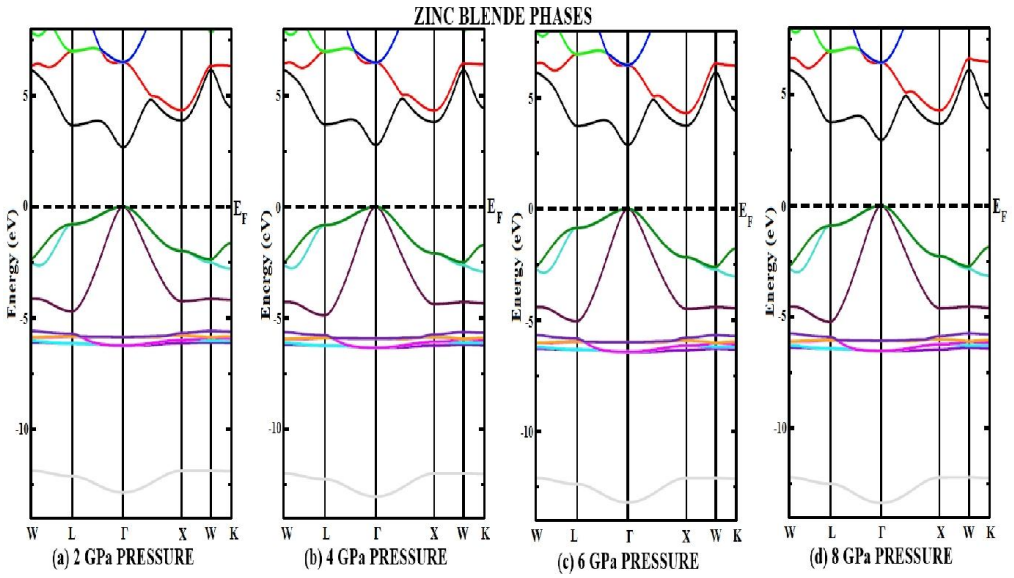

Figure 5.38. Energy band diagram ZnSe-ZB at (a) 2 GPa pressure (b) 4 GPa pressure, (c) 6 GPa pressure and (d) 8 GPa pressure

In figure 5.38 (a, b, c and d), the energy band diagrams of ZnSe-ZB at different pressures show the increase of gap at Γ- Γ point as pressure increases. Figure 5.39 shows the variation in the energy band gap between Γ-Γ point, Γ-X point and Γ-L with pressure for better understanding of the changes in the energy band gap. In figure 5.40 (a, b, c and d), the energy band diagram of ZnSe-RS phase at different pressures show the metallic nature and is observed to be retained metallic even at high pressure without much variation.

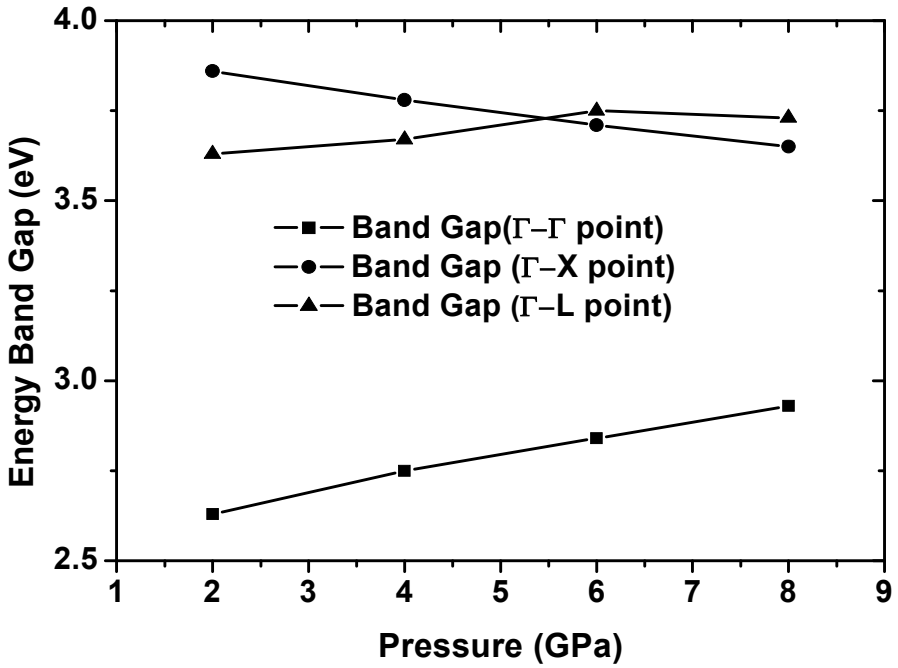

Figure 5.39. Variation of Energy band gaps of ZnSe-ZB phase with pressure.

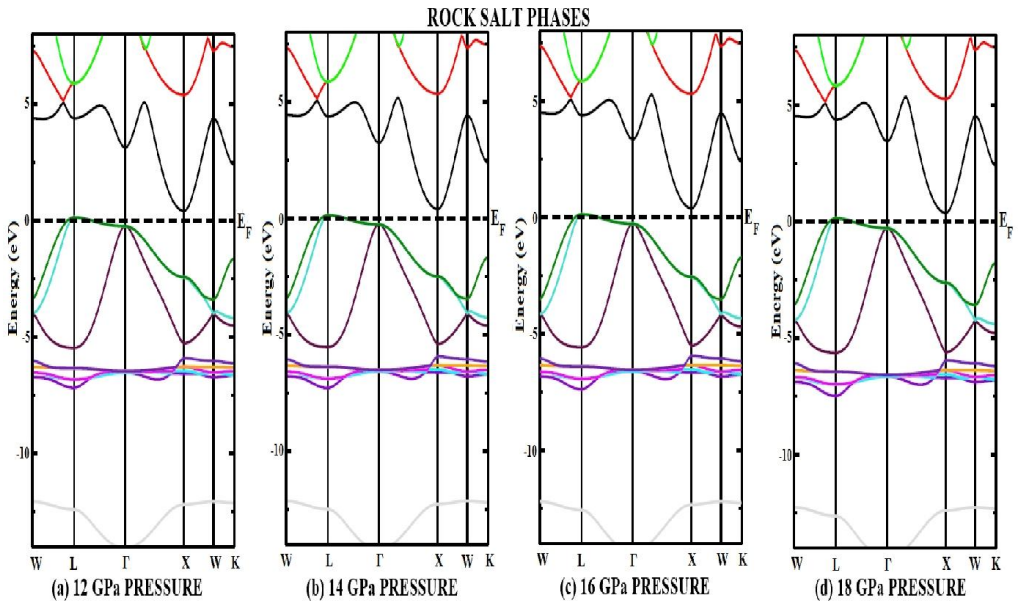

Figure 5.40. Energy band diagram ZnSe-RS at (a) 12 GPa pressure (b) 14 GPa pressure, (c) 16 GPa pressure and (d) 18 GPa pressure.

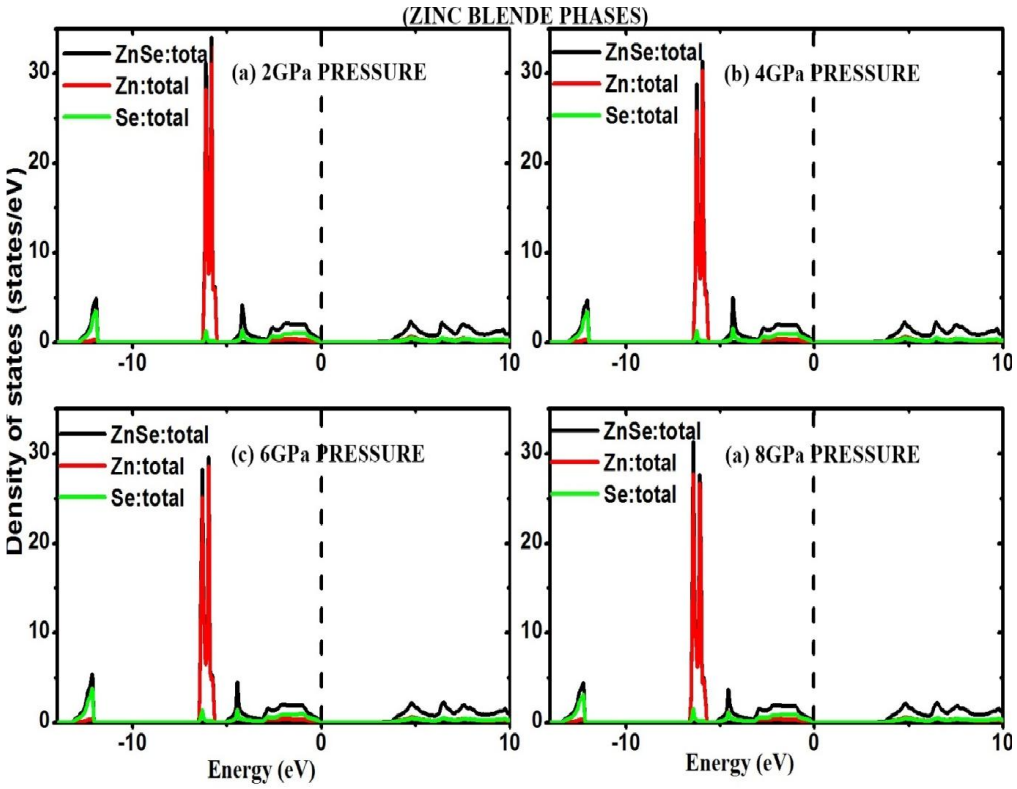

Figure 5.41. Total DOS of ZnSe-ZB at (a) 2 GPa pressure (b) 4 GPa pressure (c) 6 GPa pressure and (d) 8 GPa pressure.

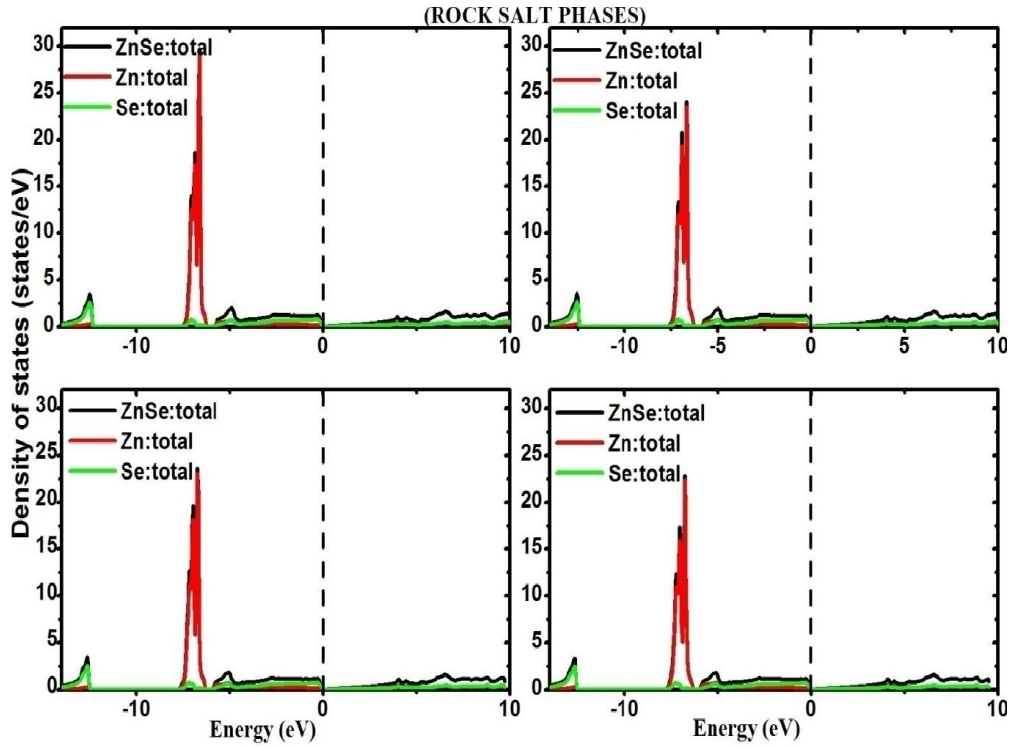

Figure 5.42. Total DOS of ZnSe-RS at (a) 12 GPa pressure (b) 14 GPa pressure (c) 16 GPa pressure and (d) 18 GPa pressure.

The total DOS of ZnSe-ZB at (a) 2 GPa pressure (b) 4 GPa pressure (c) 6 GPa pressure and (d) 8 GPa pressure (in figure 5.41) show the variation of the wide of the valence and conduction band with increase in pressure. Also the DOS plots of ZnSe-RS at (a) 12 GPa (b) 14 GPa (c) 16 GPa and (d) 18 GPa pressure (in figure 5.42) show the crossover of band at Fermi line that supports the retention of metallic nature of ZnSe-RS as observed in band diagram under pressure discussed above.

5.5. CONCLUSION

In this chapter, we have studied the structural properties of group II-VI compound semiconductors (ZnS, CdTe and ZnSe) in both ZB and RS structures. Our results are found to be in good agreement with the experimental and theoretical results.

i. The structural parameters of ZnS, CdTe and ZnSe are calculated within both the LDA and GGA as shown in table 5.1, table 5.4 and table 5.7.
ii. The structural phase transition from the zincblende (ZB) to rocksalt (RS) phase of ZnS, CdTe and ZnSe are found to occur at 17.6 GPa pressure with a volume collapse of 12.86%, 4.0 GPa pressure with a volume collapse of 20.9% and 11.5 GPa pressure with a volume collapse and 13.74% respectively.
iii. The elastic constants (C_{11}, C_{12} and C_{44}) of both the phases are calculated and found to satisfy the mechanical stability conditions The corresponding elastic parameters (Zener Anisotropy factor (A), Poisson's ratio (υ), Kleinmann parameter (ζ), B/G ratio, Young's modulus (Y) and Deby's temperature (θ_D)) are also calculated.
iv. The energy band structures of ZnS, CdTe and ZnSe at zero pressure (in ZB and RS structure) are calculated using the LDA, GGA and mBJ-GGA methods.
    - ZnS-ZB structure is a direct band gap semiconductor and energy band gap calculation with LDA and GGA shows a band gap of 1.89 eV and 1.99 eV respectively while calculation within mBJ-GGA gives a band gap of 3.5 eV which is close to experimental

result. In case of ZnS-RS, it is found to be an indirect band gap compound semiconductor of 1.1eV (within mBJ-GGA).

- CdTe in ZB phase is a direct band gap semiconductor of 1.46eV (within mBJ-GGA method) and CdTe-RS show metallic character.
- Similarly, ZnSe-ZB is found to be a direct band gap semiconductor of 2.5 eV (within mBJ-GGA method) while ZnSe-RS is metallic.

v. The DOS plots for the ZB and RS structures at zero pressure are studied within the mBJ-GGA only and at different pressures.

- In all the three compounds (ZnS-ZB, CdTe-ZB and ZnSe-ZB) we find that with increasing pressure the energy band gap between the Γ- Γ point and Γ-L increases but the gap between Γ-X are found to decrease.
- But for the RS phases, we find that the indirect band gap of ZnS and metallic nature of CdTe and ZnSe are retained even at high pressure without much variation.

Hence we conclude that the energy band gap of ZB phases of ZnS, CdTe and ZnSe are affected by pressure while the energy band gaps of the RS phases are not much affected by pressure.